Chapter 13

Designing hybrid materials

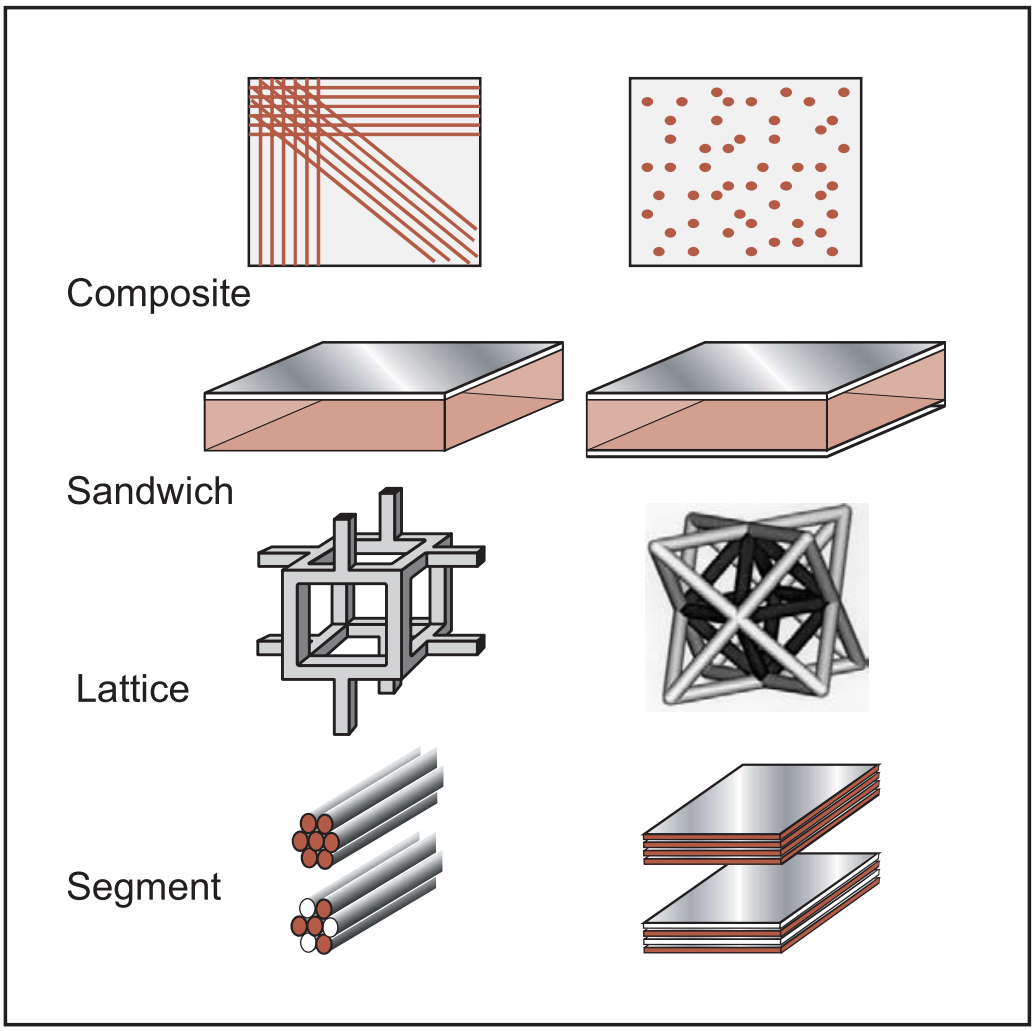

Chapter contents

13.1	Introduction and synopsis	340
13.2	Filling holes in material-property space	342
13.3	The method: "A + B + configuration + scale"	346
13.4	Composites: hybrids of type 1	348
13.5	Sandwich structures: hybrids of type 2	358
13.6	Lattices: hybrids of type 3	363
13.7	Segmented structures: hybrids of type 4	371
13.8	Summary and conclusions	376
13.9	Further reading	376

13.1 Introduction and synopsis

Why do horse breeders cross a horse with a donkey, delivering a mule? Why do farmers prefer hybrid corn to the natural strain? Mules, after all, are best known for their stubbornness, and — like hybrid corn — they cannot reproduce, so you have to start again for each generation. So — why? Because, although they have some attributes that are less good than their forebears, they have others — hardiness, strength, resistance to disease — that are better. The botanical phrase "hybrid vigor" sums it up.

So let us explore the idea of hybrid materials — combinations of two or more materials assembled in such a way as to have attributes not offered by either one alone (Figure 13.1, central circle). Like the mule, we may find that some attributes are less good (e.g. the cost), but if the ones we want are better, something is achieved. Particulate and fibrous composites are examples of one type of hybrid, but there are many others: sandwich structures, lattice structures, segmented structures, and more. Here we explore ways of designing hybrid materials, emphasizing the choice of the components, their configuration, their relative volume fraction, and their scale. The new variables expand design space, allowing the creation of new "materials" with specific property profiles. Table 13.1 lists the ingredients.

And that highlights one of the challenges. How are we to compare a hybrid like a sandwich with monolithic materials like — say — polycarbonate or titanium? To do this we must think of the sandwich not only as a hybrid with

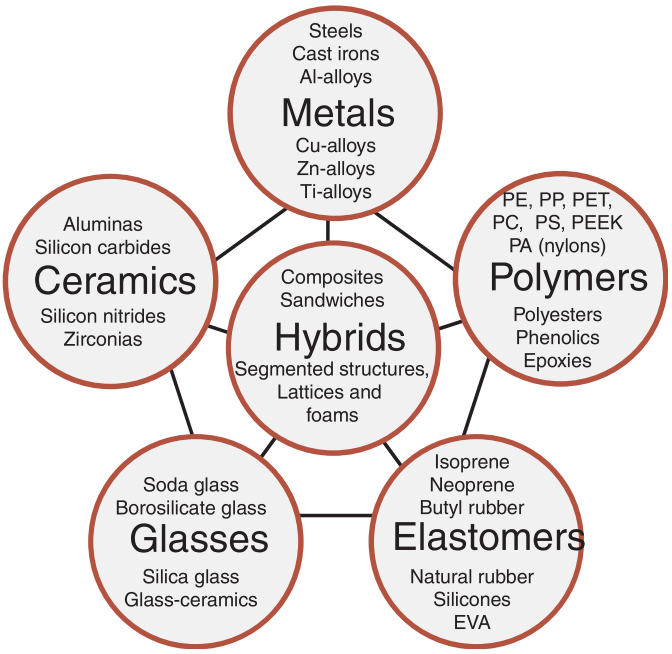

Figure 13.1 Hybrid materials combine the properties of two (or more) monolithic materials, or of one material and space. They include fibrous and particulate composites, foams and lattices, sandwiches, and almost all natural materials.

Table 13.1 Ingredients of hybrid design

Components	The choice of materials to be combined
Configuration	The shape and connectivity of the components
Relative volumes	The volume fraction of each component
Scale	The length-scale of the structural unit

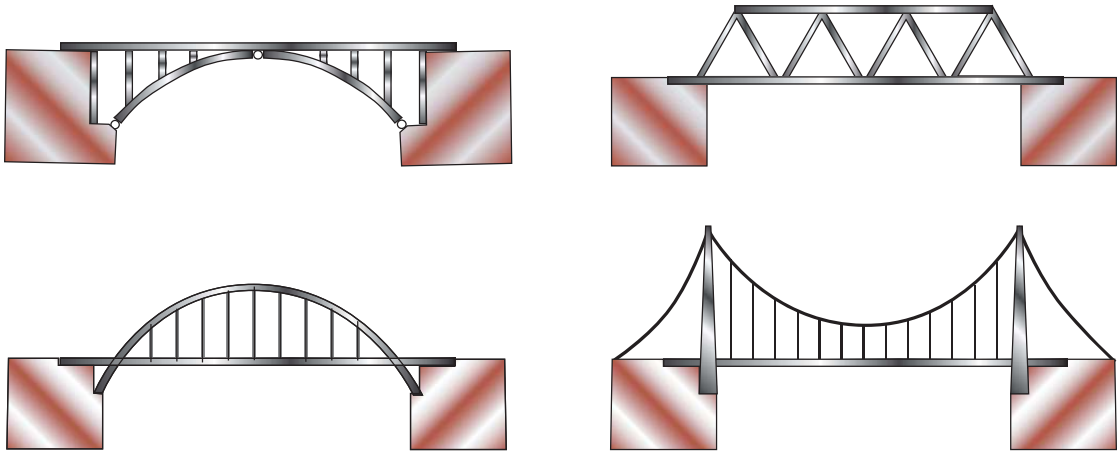

Figure 13.2 Four configurations for a bridge. The design variables describing the performance of each differ. Optimization of performance becomes possible only when a configuration has been chosen.

faces on one material bonded to a core of another, but as a "material" in its own right, with its own set of effective properties; it is these that allow the comparison.

The approach adopted here is one of breadth rather than precision. The aim is to assemble methods to allow the properties of alternative hybrids to be scanned and compared, seeking those that best meet a given set of design requirements. Once materials and configuration have been chosen, standard methods — optimization routines, finite-element analyses — can be used to refine them. But what the standard methods are *not* good at is the quick scan of alternative material–configuration combinations. That is where the approximate methods developed below, in which material and configuration become the variables, pay off.

The word "configuration" requires elaboration. Figure 13.2 shows four different configurations of a bridge. In the first all members are loaded in compression. In the second, members carry both tension and compression, depending on how the bridge is loaded. In the third and fourth, the suspension cables are loaded purely in tension. Any one of these can be optimized, but no amount of optimization will cause one to evolve into another because this

involves a discrete jump in configuration, each characterized by its own set of variables.[1]

Hybrid design has the same feature: the classes of hybrid are distinguished by their configuration. Here we focus on four classes, each with a number if discrete members. Figure 13.3 suggests what they look like; they are our bridges. To avoid a mouthful of words every time we refer to one, we use the shorthand on the left of the figure: *composite*, *sandwich*, *lattice*, and *segment*. Composites combine two solid components, one (the reinforcement) as fibers or particles, contained in the other (the matrix). Their properties are some average of those of the components, and, on a scale large compared to that of the reinforcement, they behave as if they are homogeneous. Sandwiches have one or more outer faces of one material supported by a core of another, usually a low density material—a configuration that gives an effective flexural modulus that is greater than that of either component alone. Lattices are combinations of material and space (which can, of course, contain another material). We distinguish two types: in the first the low connectivity of the struts allows them to bend when the lattice is loaded; in the other, the higher connectivity suppresses bending, forcing the struts to stretch. Segmented structures are subdivided in one, two, or three dimensions; the subdivisions both lowers the stiffness, and, by dividing the material into a number of discrete units, imparts damage tolerance. Figure 13.4 summarizes the families and the functionality each can offer. It is the starting point for configuration selection and—since each configuration offers more than one type of functionality—for multi-functional design.

The approach we adopt is to use bounding methods to estimate the properties of each configuration. With these, the properties of a given pair of materials in a given configuration can be calculated. These can then be plotted on material selection charts, which become tools for selecting both configuration and material.

13.2 Filling holes in material-property space

All the charts of Chapter 4 have one thing in common: parts of them are populated with materials and parts are not. Some parts are inaccessible for fundamental reasons that relate to the size of atoms and the nature of the forces that bind their atoms together. But other parts are empty even though,

[1] Numerical tools are emerging that allow a degree of *topological optimization*, meaning the development of a configuration. They work like this. Start with an envelope—a set of boundaries—and fill it with a homogenous "material" with a relative density initially set at 0.5, with properties that depend linearly on relative density. Impose constraints, meaning the mechanical, thermal, and other loads the structure must support, give it a criterion of excellence (more of this below) and let it condense out into regions of relative density 1 and regions where it is zero, retaining only changes that increase the measure of excellence. The method is computationally intensive but has had some success in suggesting configurations that use a material efficiently (see Further reading for more information).

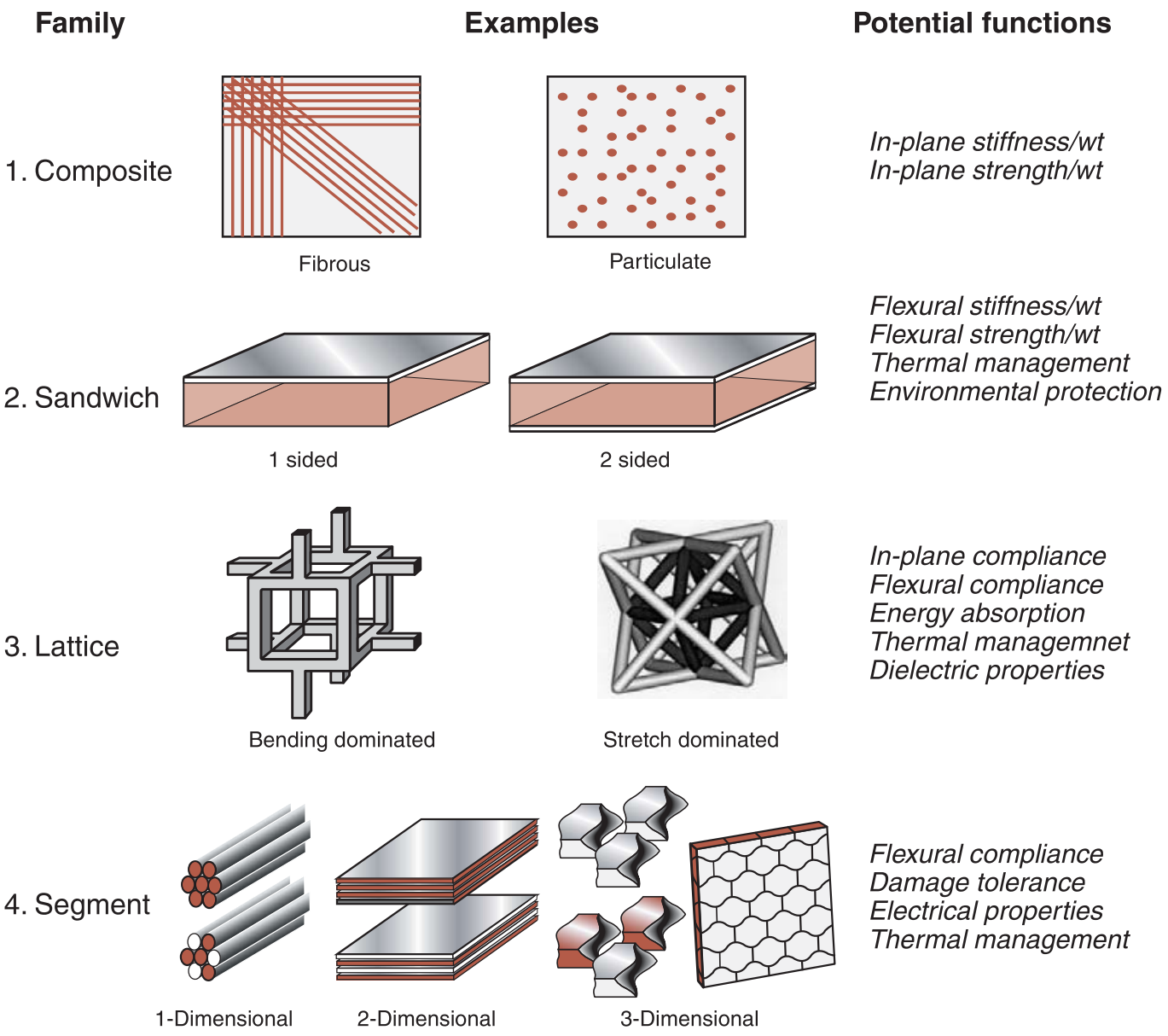

Figure 13.3 Four families of configurations of hybrid materials: composites, sandwiches, lattices, and segmented structures.

in principle, they are accessible. If these holes could be filled, the new materials that lay there could allow novel design possibilities.

One approach to this—the traditional one—is that of developing new metal alloys, new polymer chemistries and new compositions of glass and ceramic so as to extend the populated areas of the property charts, but this can be an expensive and uncertain process. An alternative is to combine two or more existing materials so as to allow a superposition of their properties—in short, to create a hybrid. The spectacular success of carbon and glass-fiber reinforced composites at one extreme, and of foamed materials at another (hybrids of material and space) in filling previously empty areas of the property charts is encouragement enough to explore ways in which such hybrids can be designed.

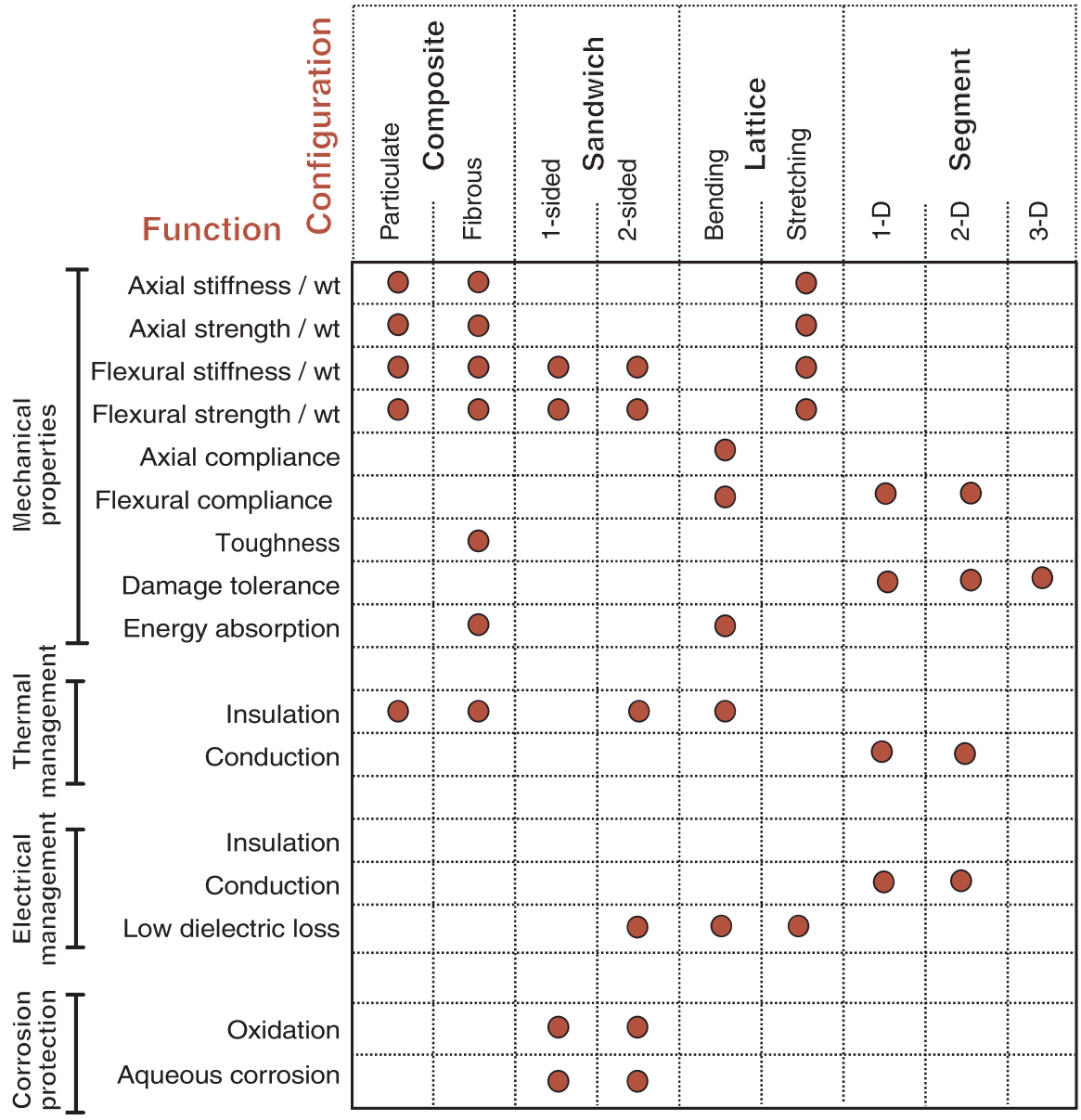

Figure 13.4 The functionality provided by each configuration.

What might we hope to achieve? Figure 13.5 shows schematically the fields occupied by two families of materials, plotted on a chart with properties P_1 and P_2 as axes. Within each field a single member of that family is identified (materials M_1 and M_2). What might be achieved by making a hybrid of the two? The figure shows four scenarios, each typical of a certain class of hybrid. Depending on the shapes of the materials and the way they are combined, we may find any one of the following.

- "The best of both" scenario (point A). The ideal, often, is the creation of a hybrid with the best properties of both components. There are examples, most commonly when a bulk property of one material is combined with the surface properties of another. Zinc coated steel has the strength and toughness of steel with the corrosion resistance of zinc. Glazed pottery

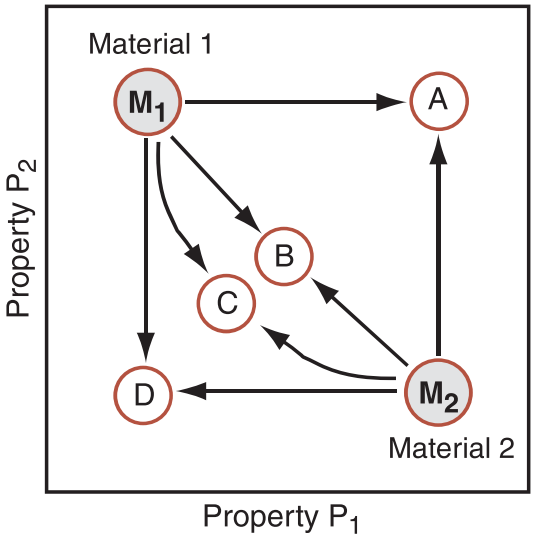

Figure 13.5 The possibilities of hybridization. The properties of the hybrid reflect those of its component materials, combined in one of several possible ways.

exploits the formability and low cost of clay with the impermeability and durability of glass.

- "The rule of mixtures" scenario (point B). When bulk properties are combined in a hybrid, as in structural composites, the best that can be obtained is often the arithmetic average of the properties of the components, weighted by their volume fractions. Thus unidirectional fiber composites have an axial modulus (the one parallel to the fibers) that lies close to the rule of mixtures.
- "The weaker link dominates" scenario (point C). Sometimes we have to live with a lesser compromise, typified by the stiffness of particulate composites, in which the hybrid properties fall below those of a rule of mixtures, lying closer to the harmonic than the arithmetic mean of the properties. Although the gains are less spectacular, they are still useful.
- "The least of both" scenario (point D). Sprinkler systems use a wax–metal hybrid designed to fail, releasing the spray, when the melting point of the lower-melting material (the wax) is exceeded.

These set certain fixed points, but the list is not exhaustive. Other combinations are possible, some giving performance that exceeds even that of point A. These will emerge below.

When is a hybrid a "material"? There is a certain duality about the way in which hybrids are thought about and discussed. Some, like filled polymers, composites or wood are treated as materials in their own right, each characterized by its own set of material properties. Others — like galvanized steel — are seen as one material (steel) to which a coating of a second (zinc) has been applied, even though if could be regarded as a new material with the strength of steel but the surface properties of zinc ("stinc", perhaps?). Sandwich panels illustrate the duality, sometimes viewed as two sheets of face-material

separated by a core material, and sometimes — to allow comparison with bulk materials — as a "material" with their own density, flexural stiffness and strength. To call any one of these a "material" and characterize it as such is a useful shorthand, allowing designers to use existing methods when designing with them. But if we are to design the hybrid itself, we must deconstruct it, and think of it as a combination of materials (or of material and space) in a chosen configuration.

13.3 The method: "A + B + configuration + scale"

First, a working definition: a hybrid material is a combination of two or more materials in a predetermined configuration, relative volume and scale, optimally serving a specific engineering purpose", which we paraphrase as "A + B + configuration + scale. Here we allow for the widest possible choice of A and B, including the possibility that one of them is a gas or simply space. These new design variables expand design-space, allowing an optimization of properties that is not possible if choice is limited to single, monolithic materials.

The basic idea, illustrated in Figure 13.6, is this. Monolithic materials offer a certain portfolio of properties on which much engineering design is based. Design requirements isolate a sector of material–property space. If this sector contains materials the requirements can be met by a single-material solution. But if the design requirements are exceptionally demanding, no single material may be found that can meet them all: the requirements lie in a hole in property

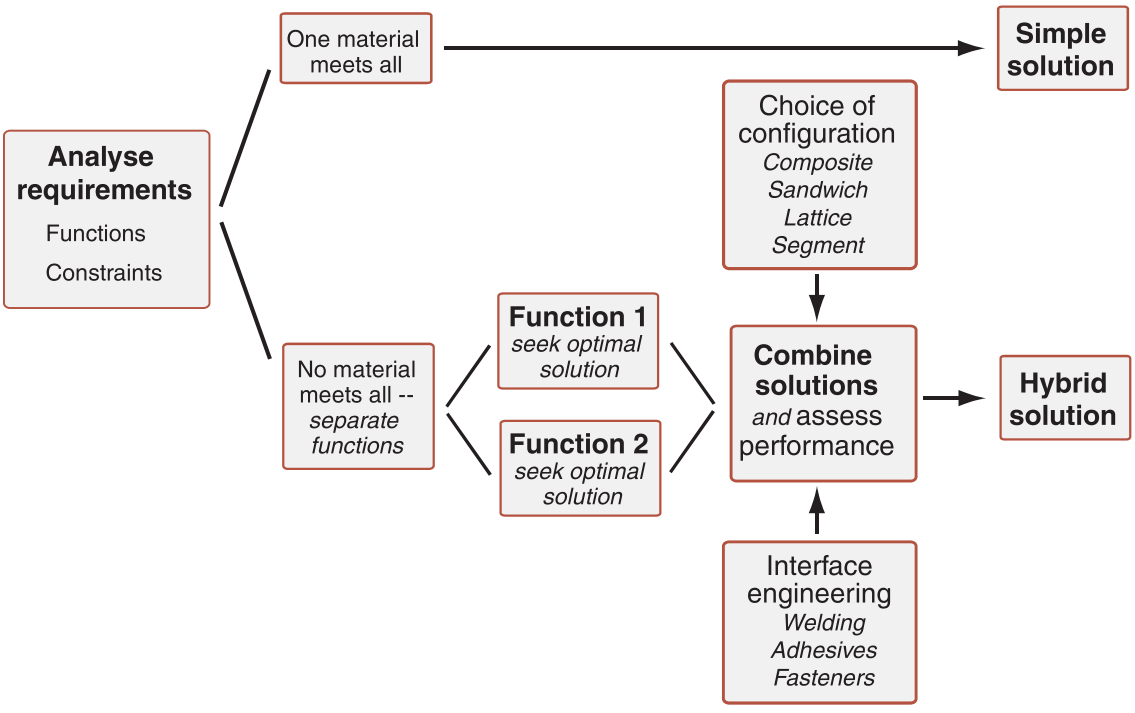

Figure 13.6 The steps in designing a hybrid to meet given design requirements.

space. Then the way forward is to identify and separate the conflicting requirements, seeking optimal material solutions for each, and then combine them in ways that retain the desirable attributes of both. The best choice is the one that ranks most highly when measured by the performance metrics that motivate the design: minimizing mass or cost, or maximizing some aspect of performance (the *criteria of excellence*). The alternative combinations are examined and assessed, using the criteria of excellence to rank them. The output is a specification of a hybrid in terms of its component materials and configurations.

Consider a simple example: materials for long-span power cables. The objectives are to minimize the electrical resistance, but at the same time to maximize the strength since this allows the greatest span. This is an example of multi-objective optimization, discussed in Chapter 9. There we mentioned the convention that each objective is expressed such that a minimum for it is sought. We thus seek materials with the lowest values of resistivity, ρ_e and the reciprocal of yield strength, $1/\sigma_y$. Figure 13.7 shows the result: materials that best meet the design requirements lie near towards the bottom left. But here there is a hole: all 1700 metals and alloys plotted here have properties that lie above the broken red trade-off line. Those with the lowest resistance — copper, aluminum, and certain of their alloys — are not very strong; the materials that are strongest — drawn carbon and low-alloy steel — do not conduct very well. Now consider a cable made by interleaving strands of copper and steel such that each occupies half the cross-section. Assuming that the steel carries no current and the copper no load (the most pessimistic scenario) the performance of the cable will lie at the point shown on the figure — it has twice the resistivity of the copper and half the strength of the steel. It lies in a part of property space that was empty, offering performance that was not previously possible. Other ratios of copper-to-steel fill other parts of the space; by varying the ratio the area shaded in gray on the figure is covered. Similar hybrids of aluminum and steel fill a different area, as is easily seen by repeating the construction using "1000 series Al alloys" in place of "OFHC copper, hard" in the combination. Their combinations of ρ_e and σ_y are less good, but they are lighter and cheaper and for this reason are widely used.

Note the method: decompose the requirements, seek good solutions for each, combine them in a chosen configuration, assess its performance, and chose the combination that offers the best.[2] But while some conflicting requirements can be met in this way, others need a more inventive approach. So the question arises: are there ways in which material hybridization can be explored systematically?

[2] The configuration we chose here (the member "multi-strand cable" from the family "segmented structures") did not require that the materials be bonded together. Other families — composites and sandwiches for example — require such bonding, and this is not always easy. Interface engineering is beyond the scope of this book, but is must be recognized that converting a hybrid concept into a reality requires the ability to create an adequate bond between the components.

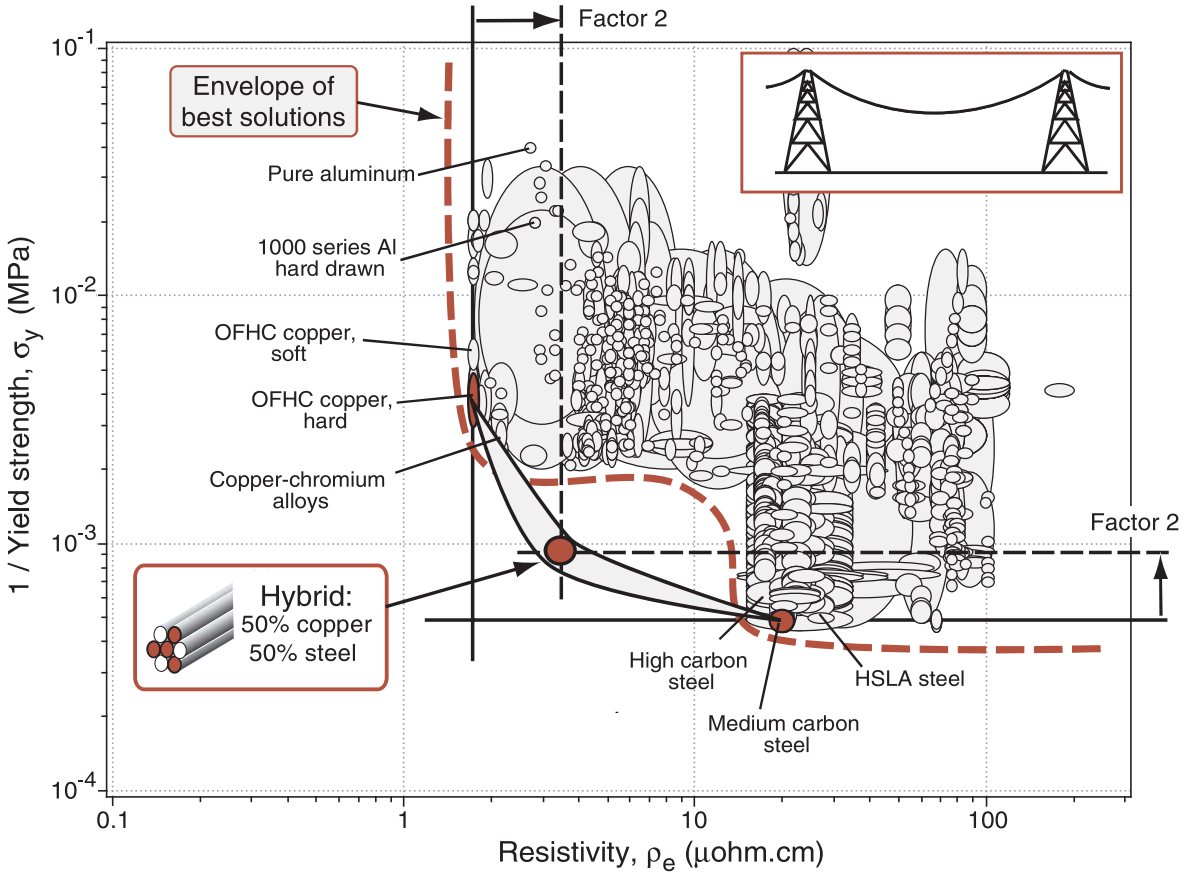

Figure 13.7 Designing a hybrid—here, one with high strength and high electrical conductivity. The figure shows the resistivity and reciprocal of tensile strength for 1700 metals and alloys. We seek materials with the lowest values of both. The construction is for a hybrid of hard-drawn OFHC copper and drawn low alloy steel, but the figure itself allows many hybrids to be investigated.

13.4 Composites: hybrids of type 1

Aircraft engineers, automobile makers, and designers of sports equipment all have one thing in common: they want materials that are stiff, strong, tough and light. The single-material choices that best achieve this are the *light alloys*: alloys based on magnesium, aluminum and titanium. Much research aims at improving their properties. But they are not all that light—polymers have much lower densities. Nor are they all that stiff—ceramics are much stiffer and, specially in the form of small particles or thin fibers, much stronger. These facts are exploited in the family of hybrids that we usually refer to as *particulate and fibrous composites*.

Any two materials can, in principle, be combined to make a composite, and they can be mixed in many geometries (Figure 13.8). In this section we restrict the discussion to *fully dense, strongly bonded, composites* such that there is no tendency for the components to separate at their interfaces when the composite

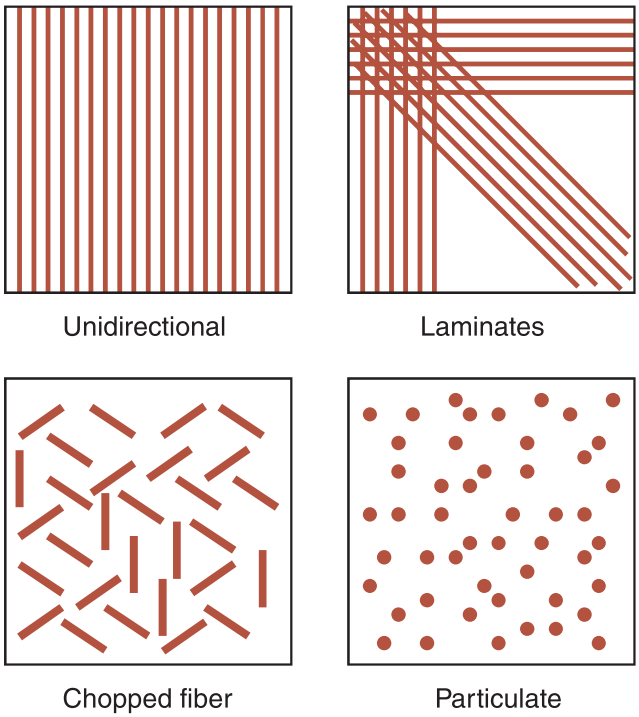

Figure 13.8 Schematic of hybrids of the composite type: unidirectional fibrous, laminated fiber, chopped fiber and particulate composites. Bounds and limits, described in the text, bracket the properties of all of these.

is loaded, and to those in which the scale of the reinforcement is large compared to that of the atom or molecule size and the dislocation spacing, allowing the use of continuum methods. Figure 13.9 shows the design variables.

On a macroscopic scale — one which is large compared to that of the components — a composite behaves like a homogeneous solid with its own set of thermo-mechanical properties. Calculating these precisely can be done, but is difficult. It is much easier to bracket them by *bounds* or *limits*: upper and lower values between which the properties lie. The term "bound" will be used to describe a rigorous boundary, one which the value of the property *cannot* — subject to certain assumptions — exceed or fall below. It is not always possible to derive bounds; then the best that can be done is to derive "limits" outside which it is *unlikely* that the value of the property will lie. The important point is that the bounds or limits bracket the properties of *all* the configurations of matrix and reinforcement shown in Figure 13.8; by using them we escape from the need to model individual geometries.

Criteria of excellence. We need criteria of excellence to assess the merit of any given hybrid. These are provided by the material indices of Chapter 5. If a possible hybrid has a value of any one of these that exceed those of existing materials, it achieves our goal.

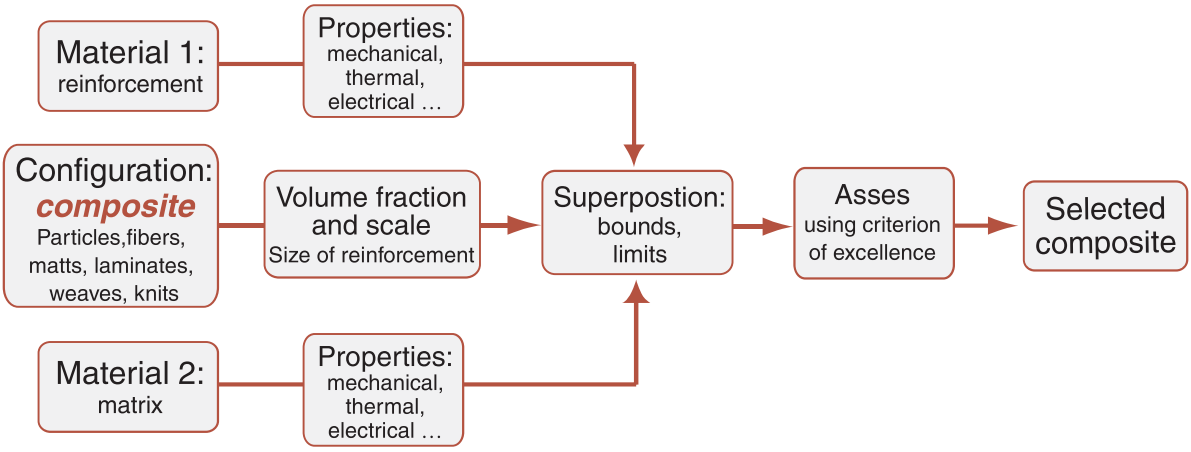

Figure 13.9 Composites: the design variables. They include the choice of material for the matrix and the reinforcement, and its shape, scale and configuration.

Density. When a volume fraction f of a reinforcement r (density ρ_r) is mixed with a volume fraction $(1-f)$ of a matrix m (density ρ_m) to form a composite with no residual porosity, the composite density $\tilde{\rho}$ is given exactly by a rule of mixtures (an arithmetic mean, weighted by volume fraction):

$$\tilde{\rho} = f\rho_{\mathrm{r}} + (1-f)\rho_{\mathrm{m}} \tag{13.1}$$

The geometry or shape of the reinforcement does not matter except in determining the maximum packing-fraction of reinforcement and thus the upper limit for f.

Modulus. The modulus of a composite is bracketed by the well-known Voigt and Reuss bounds. The upper bound, $\widetilde{E}_{\mathrm{u}}$, is obtained by postulating that, on loading, the two components suffer the same strain; the stress is then the volume-average of the local stresses and the composite modulus follows a rule of mixtures:

$$\widetilde{E}_{\mathrm{u}} = fE_{\mathrm{r}} + (1-f)E_{\mathrm{m}} \tag{13.2}$$

Here E_r is the Young's modulus of the reinforcement and E_{m} that of the matrix. The lower bound, $\widetilde{E}_{\mathrm{L}}$, is found by postulating instead that the two components carry the same stress; the strain is the volume-average of the local strains and the composite modulus is

$$\widetilde{E}_{\mathrm{L}} = \frac{E_{\mathrm{m}}E_{\mathrm{r}}}{fE_{\mathrm{m}} + (1-f)E_{\mathrm{r}}} \tag{13.3}$$

More precise bounds are possible but the simple ones are adequate to illustrate the method.

Strength. As the load on a composite is increased, load is redistributed between the components until general yield or fracture of one component occurs. Beyond this point the composite has suffered permanent deformation or damage; we define it as strength of the composite. The composite is strongest if both components reach their failure state simultaneously since if one fails before the other the weaker determines the strength. Thus the upper bound is, as with modulus, a rule of mixtures

$$(\tilde{\sigma}_f)_u = f(\sigma_f)_r + (1-f)(\sigma_f)_m \tag{13.4}$$

where $(\sigma_f)_m$ is the strength of the matrix and $(\sigma_f)_r$ is that of the reinforcement.

A lower bound is more difficult. The literature contains many calculations for special cases: reinforcement by unidirectional fibers, or by a dilute dispersion of spheres. We wish to avoid models which require detailed knowledge of how a particular architecture behaves, and seek a less restrictive lower limit. One, consistent with the requirement that the components of the composite do not separate at their interfaces, is developed in the references listed under Further reading. It describes a "worst case": a continuous, ductile, matrix containing strong reinforcing particles; the lower limit for the composite strength is then the yield strength of the matrix enhanced slightly by the plastic constraint imposed by the reinforcement

$$(\tilde{\sigma}_f)_L = (\sigma_f)_m\left(1+\frac{1}{16}\left(\frac{f^{1/2}}{1-f^{1/2}}\right)\right) \tag{13.5}$$

The consequence of this choice is that the bounds are wide, but—as the examples of Chapter 14 will show—they still allow useful conclusions to be reached.

Specific heat. The specific heats of solids at constant pressure, C_p, are almost the same as those at constant volume, C_v. If they were identical, the heat capacity per unit volume of a composite would, like the density, be given exactly by a rule-of-mixtures

$$\rho\tilde{C}_p = f\rho_r(C_p)_r + (1-f)\rho_m(C_p)_m \tag{13.6}$$

where $(C_p)_r$ is the specific heat of the reinforcement and $(C_p)_m$ is that of the matrix (the densities enter because the units of C_p are J/kg.K). A slight difference appears because thermal expansion generates a misfit between the components when the composite is heated; the misfit creates local pressures on the components and thus changes the specific heat. The effect is very small and need not concern us further.

Thermal expansion coefficient. The thermal expansion of a composite can, in some directions, be greater than that of either component, in others, less. This is because an elastic constant—Poisson's ratio—couples the principal elastic strains; if the matrix is prevented from expanding in one direction

(by embedded fibers, for instance) then it expands more in the transverse directions. For simplicity we shall use the approximate lower bound

$$\tilde{\alpha}_L = \frac{E_r \alpha_r f + E_m \alpha_m (1-f)}{E_r f + E_m (1-f)} \tag{13.7}$$

(it reduces to the rule of mixtures when the moduli are the same) and the upper bound

$$\tilde{\alpha}_u = f\alpha_r(1+\nu_r) + (1-f)\alpha_m(1+\nu_m) - \alpha_L[f\nu_r + (1-f)\nu_m] \tag{13.8}$$

where α_r and α_m are the two expansion coefficients and ν_r and ν_m the Poisson's ratios.

Thermal conductivity. The thermal conductivity determines heat flow at steady rate. A composite of two materials, bonded to give good thermal contact, has a thermal conductivity λ that lies between those of the individual components, λ_m and λ_r. Not surprisingly, a composite containing parallel continuous fibers has a conductivity, parallel to the fibers, given by a rule-of-mixtures

$$\tilde{\lambda}_u = f\lambda_r + (1-f)\lambda_m \tag{13.9}$$

This is an upper bound: in any other direction the conductivity is lower. The transverse conductivity of a parallel-fiber composite (again assuming good bonding and thermal contact) lies near the lower bound first derived by Maxwell

$$\tilde{\lambda}_L = \lambda_m \left(\frac{\lambda_r + 2\lambda_m - 2f(\lambda_m - \lambda_r)}{\lambda_r + 2\lambda_m + f(\lambda_m - \lambda_r)} \right) \tag{13.10}$$

Particulate composites, too, have a conductivity near this lower bound. Poor interface conductivity can make λ drop below it. Debonding or an interfacial layer between reinforcement and matrix can cause this; so, too, can a large difference of modulus between reinforcement and matrix (because this reflects phonons, creating an interface impedance) or a structural scale which is shorter than the phonon wavelengths.

Thermal diffusivity. The thermal diffusivity

$$a = \frac{\lambda}{\rho C_p}$$

determines heat flow when conditions are transient, that is, when the temperature field changes with time. It is formed from three of the earlier

properties: λ, ρ, and C_p. The second and third of these are given exactly by equations (13.1) and (13.6), allowing the diffusivity to be expressed as

$$\tilde{a} = \frac{\tilde{\lambda}}{f\rho_r(C_p)_r + (1-f)\rho_m(C_p)_m} \tag{13.11}$$

Its upper and lower bounds are found by substituting those for $\tilde{\lambda}$ (equations (13.9) and (13.10)) into this equation.

Dielectric constant. The dielectric constant $\tilde{\varepsilon}$ is given by a rule of mixtures

$$\tilde{\varepsilon} = f\varepsilon_r + (1-f)\varepsilon_m \tag{13.12}$$

where ε_r is the dielectric constant of the reinforcement and ε_m that of the matrix.

Electrical conductivity. When the electrical conductivities κ of the components of a composite are of comparable magnitude, bounds for the electrical conductivity are given by those for thermal conductivity with λ replaced by the κ. When, instead, they differ by many orders of magnitude (a metallic powder dispersed in an insulating polymer, for instance) questions of percolation arise. They are considered below.

To see how the bounds are used, consider the following three examples.

Composite design for stiffness at minimum mass

We seek a composite offering high stiffness-to-weight in structures subjected to bending loads. The performance of a material as a light, stiff, beam is measured by the index $E^{1/2}/\rho$ derived in Chapter 5. Imagine, as an example, that the beam is at present made of an aluminum alloy. Beryllium is both lighter and stiffer than aluminum; ceramics are stiffer, but not all are lighter. What can hybrids of aluminum with one of these offer?

Figure 13.10 is a small part of the $E-\rho$ property chart. Three groups of materials are shown: aluminum and its alloys, alumina (Al_2O_3) and beryllium (Be). Composites made by mixing them have densities given exactly by equation (13.1) and moduli that are bracketed by the bounds of equations (13.2) and (13.3). Both of these moduli depend on volume fraction of reinforcement, and through this, on density. Upper and lower bounds for the modulus–density relationship can thus be plotted onto the $E-\rho$ chart using volume fraction f as a parameter, as shown in Figure 13.10. Any composite made by combining aluminum with alumina will have a modulus contained in the envelope for Al–Al_2O_3; the same for Al–Be. Fibrous reinforcement gives a longitudinal modulus (that parallel to the fibers) near the upper bound; particulate reinforcement or transversely loaded fibers give moduli near the lower one.

Superimposed on Figure 13.10 is a grid showing the criterion of excellence $E^{1/2}/\rho$. The bound-envelope for Al–Be composites extends almost normal to the

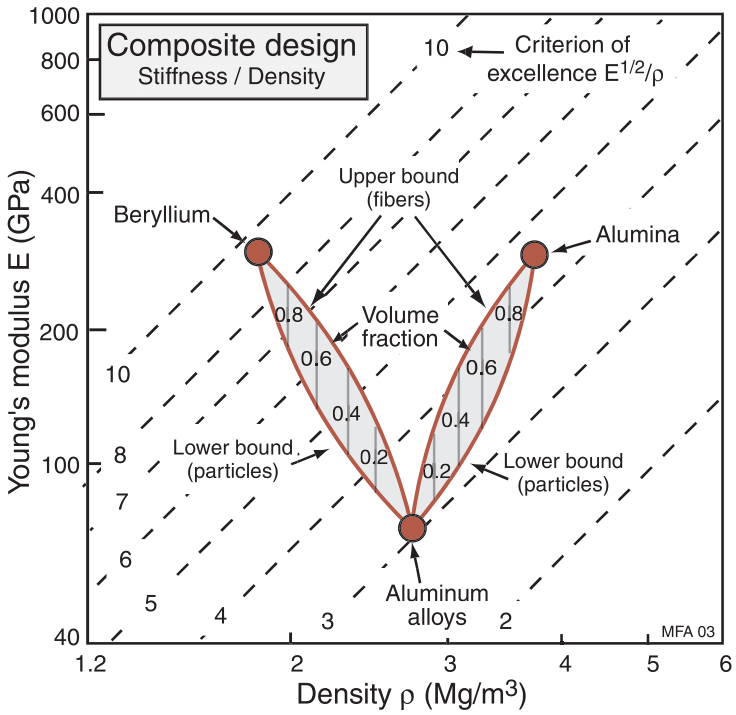

Figure 13.10 Part of the $E - \rho$ property chart, showing aluminum alloys, beryllium and alumina (Al_2O_3). Bounds for the moduli of hybrids made by mixing them are shown. The diagonal contours plot the criterion of excellence, $E^{1/2}/\rho$.

grid, while that for Al–Al_2O_3 lies at a shallow angle to it. Beryllium fibers improve performance (as measured by $E^{1/2}/\rho$) roughly four times as much as alumina fibers do, for the same volume fraction. The difference for particulate reinforcement is even more dramatic. The lower bound for Al–Be lies normal to the contours: 30% of particulate beryllium increases $E^{1/2}/\rho$ by a factor of 1.5. The lower bound for Al–Al_2O_3 is, initially, parallel to the $E^{1/2}/\rho$ grid: 30% of particulate Al_2O_3 gives almost no gain. The underlying reason is clear: both beryllium and Al_2O_3 increases the modulus, but only beryllium decreases the density; the criterion of excellence is more sensitive to density than to modulus.

Composite design for controlled thermal response

Thermo-mechanical design involves the specific heat, C_p, the thermal expansion, α, the conductivity, λ, and the diffusivity, a. These composite properties are bounded by equations (13.6)–(13.11). They are involved in a number of indices. One is the criterion for minimizing thermal distortion derived in Chapter 6, section 6.16: it is that of maximizing the index λ/α.

Figure 13.11 shows a small part of the $\alpha - \lambda$ materials selection chart, with a grid of lines of the index λ/α superimposed on it. Three groups of materials are shown: aluminum alloys, boron nitride (BN) and silicon carbide (SiC). The thermal properties of Al–BN and Al–SiC are bracketed by lines which

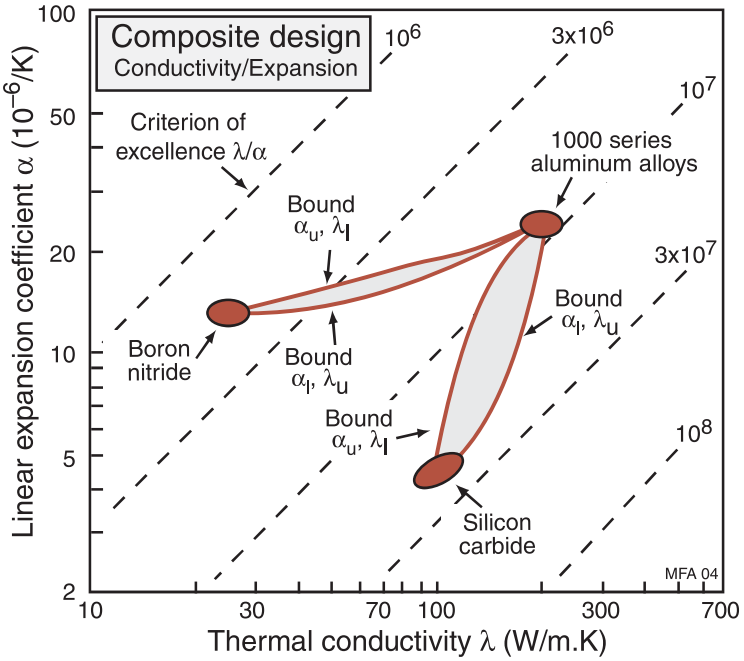

Figure 13.11 A part of expansion-coefficient/conductivity space showing aluminum alloys, boron nitride and silicon carbide. The properties of Al–BN and Al–SiC composites are bracketed by the bounds of equations (13.7)–(13.10). The Al–SiC composites enhance performance, the Al–BN composites reduce it.

show the bounding equations.[3] The plot reveals immediately that SiC reinforcement in aluminum increases performance (as measured by λ/α); reinforcement with BN decreases it.

Similar methods can be used to select materials for optimum strength, and for tailored values of thermal properties. The properties of specific composites can, of course, be computed in conventional ways. The advantage of this graphical approach is the breadth and freedom of conceptual thinking that it allows and the ease of comparison of possible new hybrids with the population of existing materials.

Creating anisotropy

The elastic and plastic properties of bulk monolithic solids are frequently anisotropic, but weakly so — the properties do not depend strongly on direction. Hybridization gives a way of creating controlled anisotropy, and it can be large. We have already seen an example in Figure 13.10, which shows the upper and lower bounds for the moduli of composites. The longitudinal properties of unidirectional long-fiber composites lie near the upper bound, the transverse properties near the lower one. The vertical width of the band in between them

[3] Both α and λ have upper and lower bounds (unlike ρ in the previous example) so there are four possible combinations for each material pair. Those shown in the figure are the outermost pair of the four.

measures the anisotropy. A unidirectional continuous-fiber composite has an anisotropy ratio R_a given by the ratio of the bounds — in this example

$$R_a = \frac{(fE_r + (1-f)E_m)^2}{E_r E_m} \tag{13.13}$$

In Figure 13.10 the maximum R_a is only 1.5. A more dramatic example involving thermal properties is given in Chapter 14.

Percolation: properties that switch on and off

So far we have explored "well-behaved" properties — those that can be treated by methods of continuum mechanics. Equations (13.1)–(13.11) are continuum limits, and are independent of the scale of the reinforcement. Not all composites behave like that.

Figure 13.12, a chart of electrical resistivity against elastic stiffness (here measure by Young's modulus), has an enormous hole. Materials that conduct well are stiff; those that are flexible are insulators. Consider designing materials to fill the hole; to be more specific, consider designing one that has low modulus, can be molded like a polymer, and is a good electrical conductor. Such materials find application in anti-static clothing and mats, as pressure sensing elements, even as solder-less connections.

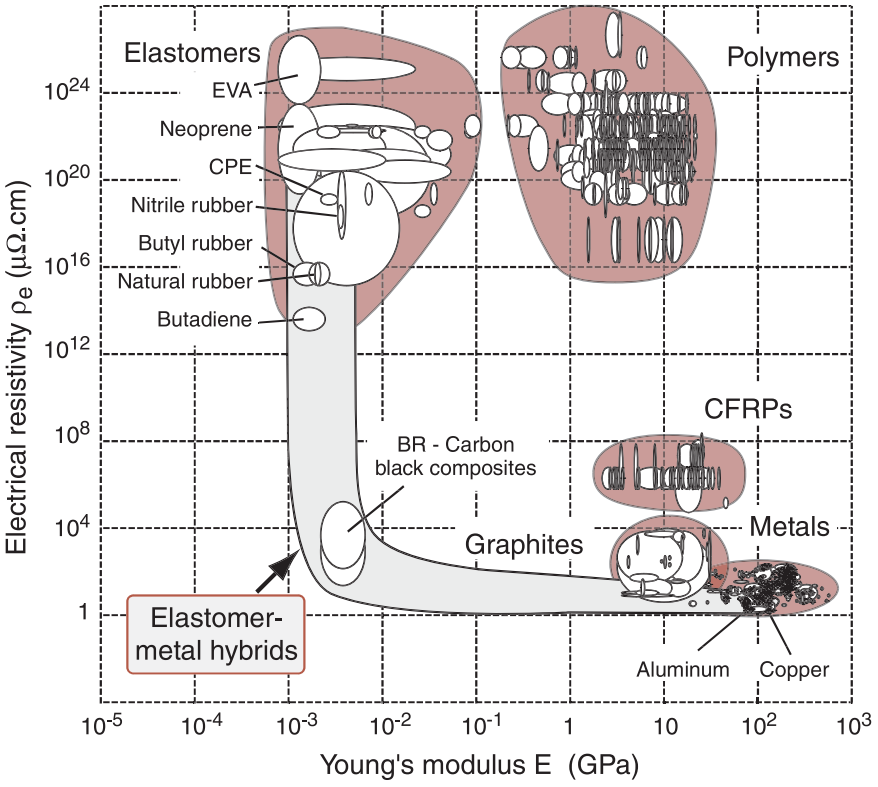

Figure 13.12 When conducting particles or fibers are mixed into an insulating elastomer, a hole in material property space is filled. Carbon-filled butyl rubbers lie in this part of the space.

Next Page

Metals, carbon, and some carbides and intermetallics are good conductors, but they are stiff and cannot be molded. Thermoplastic and thermosetting elastomers can be molded and are flexible, but they do not conduct. How are they to be combined? Metal coating of polymers is workable if the product will be used in a protected environment, but coatings are easily damaged. If a robust, flexible, product is needed, bulk rather than surface conduction is essential. This can be achieved by mixing conducting particles into the polymer.

To understand how to optimize this we need the concept of *percolation*. Think of mixing conducting and insulating spheres of the same size to give a large array. If there are too few conducting spheres for them to touch, the array is obviously an insulator. If each conducting sphere contacts just one other, there is still no connecting path. If, on average, each touched two, there is still no path. Adding more spheres gives larger clusters, but they can be large yet still discrete. For bulk conduction we need *connectivity*: the array first becomes a conductor when a single trail of contacts links one surface to the other, that is, when the fraction p of conducting spheres reaches the *percolation threshold*, p_c. Percolation problems are easy to describe but difficult to solve. Research since 1960 has provided approximate solutions to most of the percolation problems associated with the design of hybrids (see Further reading for a review). For simple cubic packing $p_c = 0.248$, for close packing $p_c = 0.180$. For a random array it is somewhere in between — approximately 0.2.[4]

Make the spheres smaller and the transition is smeared out. The percolation threshold is still 0.2, but the first connecting path is now thin and extremely devious — it is the only one, out of the vast number of almost complete paths, that actually connects. Increase the volume fraction and the number of conducting paths increases initially as $(p - p_c)^2$, then linearly, reverting to a rule of mixtures. If the particles are very small, as much as 40% may be needed to give good conduction. But a loading of 40% seriously degrades the moldability and compliance of the polymer.

Shape gives a way out. If the spheres are replaced by fibers, they touch more easily and the percolation threshold falls. If their aspect ratio is $\beta = L/d$ (where L is the fiber length, d the diameter) then, empirically, the percolation threshold falls from p_c to roughly $p_c/\beta^{1/2}$. Figure 13.12 shows the area of the property chart where metal–elastomer hybrids lie. With sufficient aspect ratio the percolation threshold falls to a few percentage.

The concept of percolation is a necessary tool in designing hybrids. Electrical conductivity works that way; so too does the passage of liquids through foams or porous media — no connected paths, and no fluid flows; just one (out of a million possibilities) and there is a leak. Add a few more connections and there is a flood. Percolation ideas are particularly important in understanding the transport properties of hybrids: properties that determine the flow of

[4] These results are for infinite, or at least very large, arrays. Experiments generally give values in the range 0.19–0.22, with some variability because of the finite size of the samples.

Previous Page

electricity or heat, of fluid, or of flow by diffusion, specially when the differences in properties of the components are extreme. Most polymers differ from metals in their electrical conductivity by a factor of about 10^{20}. It is then that single connections really matter.

Percolation influences mechanical properties too, particularly when mechanical connection is important, as in arrays of loose powders or fibers. If there are no bonds between the particles or fibers, the array has no tensile stiffness or strength. If each particle is bonded to one other, or to several forming discrete clusters, there is still no tensile stiffness or strength. These only appear when there are connected paths running completely through the array. The plasticity of 2-phase hybrids, too, can be viewed as a percolation problem. Plasticity may start in one phase at a low stress, allowing patches of slip to form, but full plasticity requires that the slip patches link to give connected paths through the entire cross section of the sample.

13.5 Sandwich structures: hybrids of type 2

A sandwich panel epitomizes the concept of a hybrid. It combines two materials in a specified geometry and scale, configured such that one forms the faces, the other the core, to give a structure of high bending stiffness and strength at low weight (Figure 13.13). The separation of the faces by the core increases the moment of inertia of the section, *I*, and its section modulus, *Z*, producing a structure that resists bending and buckling loads well. Sandwiches are used where weight-saving is critical: in aircraft, trains, trucks and cars, in portable structures, and in sports equipment. Nature, too, makes use of sandwich designs: sections through the human skull, the wing of a bird and the stalk and leaves of many plants show a low-density foam-like core separating solid faces.

The faces, each of thickness *t*, carry most of the load, so they must be stiff and strong; and they form the exterior surfaces of the panel so they must tolerate the environment in which it operates. The core, of thickness *c*, occupies most of the volume, it must be light, and stiff and strong enough to carry the shear stresses necessary to make the whole panel behave as a load bearing

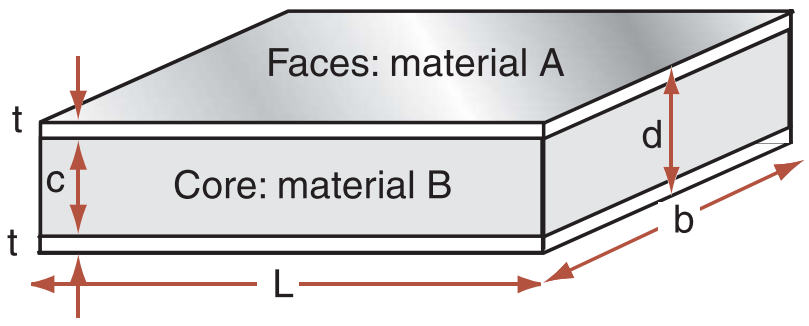

Figure 13.13 The ultimate light, stiff hybrid: the sandwich panel.

unit, but if the core is much thicker than the faces these stresses are small. Figure 13.14 indicates the design variables.

A sandwich as a "material". So far we have spoken of the sandwich as a structure: faces of material A supported on a core of material B, each with its own density and modulus. But we can also think of it as a material with its own set of properties, and this is useful because it allows comparison with more conventional materials. Density is easy—it is given exactly by the rule of mixtures, equation (13.1), with f replaced by $2t$ and $(1-f)$ replaced by c (a substitution we shall use throughout this section):

$$\tilde{\rho} = \frac{2t}{d}\rho_f + \left(1 - \frac{2t}{d}\right)\rho_c \tag{13.14}$$

Mechanical properties. Sandwich panels are designed to be stiff and strong in bending. In thinking of the panel as a "material" we must therefore distinguish the in-plane modulus and strength from those in bending. The in-plane modulus, $\tilde{E}_{//}$, is given exactly by the rule of mixtures, equation (13.2). An upper bound for the in-plane strength is found by postulating that faces and core reach yield or failure together, giving once more the rule of mixtures of equation (13.4). A lower bound is found by proposing that the first yield or failure of either faces or core constitutes failure, giving

$$\tilde{\sigma}_{f,L} = \text{Least of}\left[\left(\frac{\tilde{E}_{//}}{E_f}(\sigma_y)_f\right), \left(\frac{\tilde{E}_{//}}{E_c}(\sigma_y)_c\right)\right] \tag{13.15}$$

Here $(\sigma_y)_f$ is the elastic limit of the material of the faces, and $(\sigma_y)_c$ that of the core.

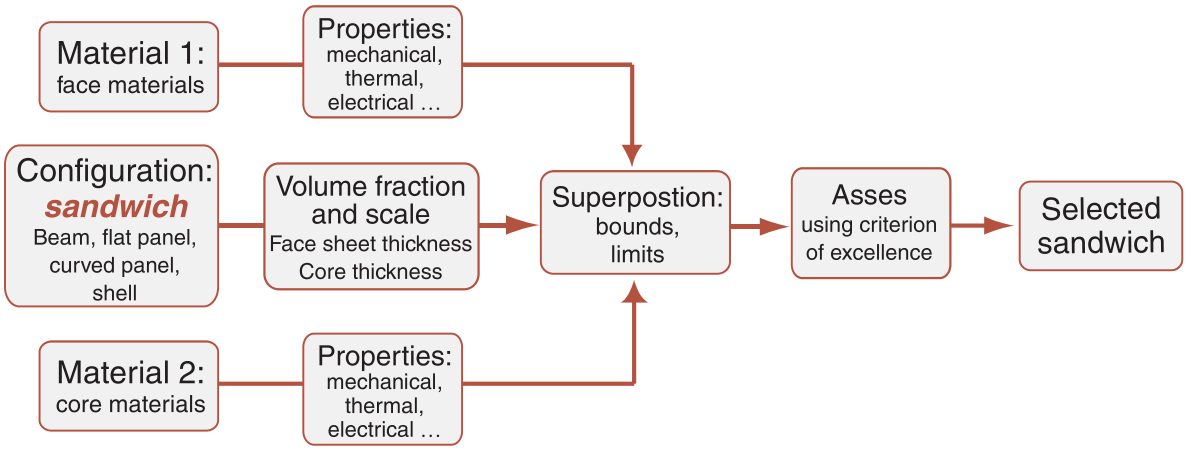

Figure 13.14 Sandwich panels: the design variables. They include the material choice for faces and core, their thicknesses, and the curvature of the panel itself.

The flexural properties are quite different. The bending stiffness of the panel per unit width, S_w is given by

$$S_w = (EI)_{sand} = \left[\frac{1}{12}(d^3 - c^3)E_f\right]\left\{\frac{1}{1 + BE_f tc/2G_c L^2}\right\}$$
$$\text{or} \quad S_w = (EI)_{sand} = \left[\frac{1}{12}(d^3 - c^3)E_f\right]K_s \tag{13.16}$$

where the dimensions, d, c, t, and L are identified in Figure 13.13, E_f is Young's modulus of the face sheets and G_c is the shear modulus of the core. The numerical constant B depends only on the way the panel is loaded—Figure 13.15 gives values. Equation (13.16) has two terms. The first, in square brackets, is the stiffness if bending were the only mode of deformation. The second, in curly brackets, is the knock-down in stiffness (condensed here into the symbol K_s) caused by shear in the core. If the core adequately resists shear, the second term reduces to unity. To think of the sandwich as a material, we define an effective flexural modulus $\widetilde{E}_{flex}$ equal to the modulus of a *homogeneous* material with the same bending stiffness as the sandwich, requiring that

$$(EI)_{sand} = \widetilde{E}_{flex}\frac{d^3}{12}$$

from which

$$\widetilde{E}_{flex} = \left(1 - \frac{c^3}{d^3}\right)E_f K_s = \left(1 - \left(1 - \frac{2t}{d}\right)^3\right)E_f K_s \tag{13.17a}$$

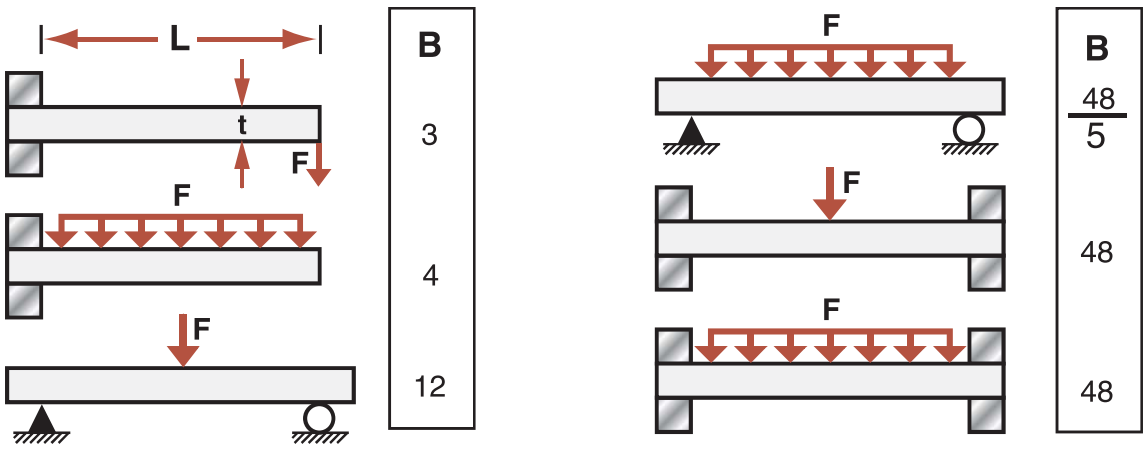

Figure 13.15 Values for the constant B in the equation for the bending stiffness of sandwich panels.

($d^3/12$ is the second moment of area per unit width of a homogeneous panel of thickness d). When $t \ll d$ and $K_s \approx 1$, this reduces to

$$\tilde{E}_{\text{flex}} \approx \frac{6t}{d} E_f \tag{13.17b}$$

It leads to the performance shown in Figure 13.16, which has been constructed in the same way as Figure 13.10. It shows the modulus and density of A+B hybrids. The shaded band is bounded by the upper and lower bounds of equations (13.1)–(13.3), describing particulate and fibrous composites. The flexural performance of the sandwich is shown as a dashed line. At its mid-section the modulus of the sandwich lies a factor 3 above the upper bound rule of mixtures of equation (13.2). The criterion of excellence for a panel of minimum weight with prescribed bending stiffness is that of maximizing $E_{1/3}/\rho$. Contours of this criterion are plotted as diagonal lines on the figure, increasing towards the top left. The sandwich out-performs all alternative hybrids of A + B.

The bending strength or *modulus of rupture* of a sandwich, $\tilde{\sigma}_{\text{MoR}}$, can be bracketed by limits. An upper limit is given by requiring that the faces and core yield simultaneously, when

$$\tilde{Z}\tilde{\sigma}_{\text{MoR}} = \frac{1}{6d}(d^3 - c^3)\sigma_f + \frac{c^2}{6}\sigma_c \tag{13.18}$$

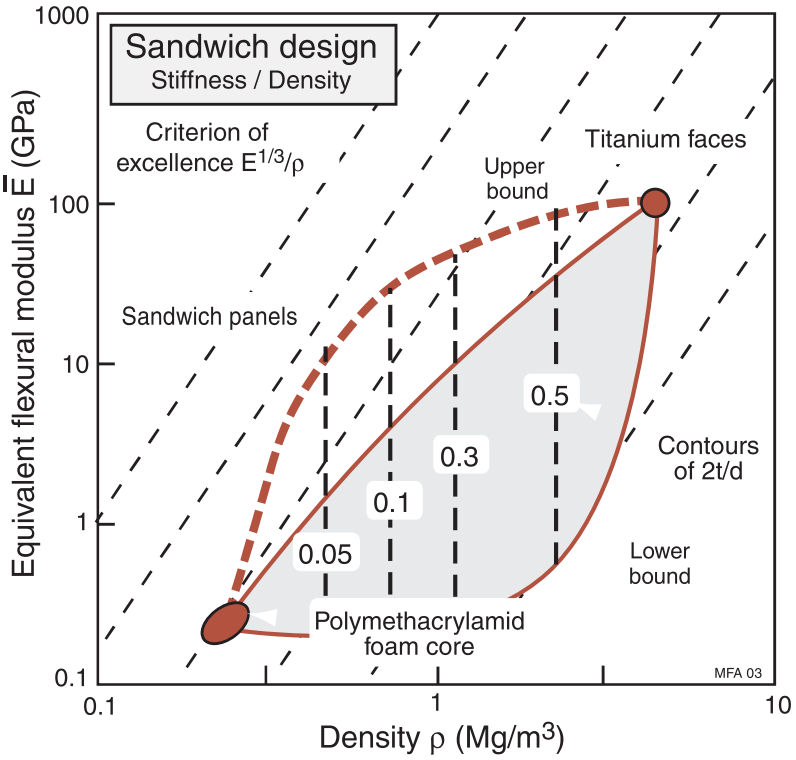

Figure 13.16 The performance of a sandwich structure compared with that of a composite made from the same two materials. The sandwich is more efficient if bending than even the best composites.

But $\tilde{Z}$ is just the section modulus of a homogenous section of thickness d (with value $d^2/6$), so that the upper bound for the panel strength $(\tilde{\sigma}_{\mathrm{MoR}})_{\mathrm{ub}}$ is given by

$$\begin{aligned}(\tilde{\sigma}_{\mathrm{MoR}})_{\mathrm{u}} &= \left(1-\frac{c^3}{d^3}\right)\sigma_{\mathrm{f}}+\frac{c^2}{d^2}\sigma_{\mathrm{c}} \\ &= \left(1-\left(1-\frac{2t}{d}\right)^3\right)\sigma_{\mathrm{f}}+\left(1-\frac{2t}{d}\right)^2\sigma_{\mathrm{c}}\end{aligned} \tag{13.19}$$

The panel can fail in many other ways, illustrated by Figure 13.17, although a well-designed panel should not do so. Each of these can be modeled—such models can be found in the texts listed under Further reading. The bending strength of the panel is determined by the weakest of these competing mechanisms. Some, such a bond failure, can reduce the strength almost to zero. We are forced to accept that there is no lower bound on strength. This is not as serious as it sounds since the upper bound is realizable, and gives a realistic basis for comparing the panel with other materials.

Thermal properties. Thermal properties are treated in a similar way. The specific heat, C_{p} follows a rule of mixtures, equation (13.6). The in-plane thermal conductivity $\lambda_{//}$, too, follows such a rule—equation (13.9). The through-thickness conductivity, $\lambda_{\perp}$, is given by the harmonic mean

$$\tilde{\lambda}_{\perp}=\left(\frac{2t/d}{\lambda_{\mathrm{f}}}+\frac{(1-2t/d)}{\lambda_{\mathrm{c}}}\right)^{-1} \tag{13.20}$$

Thermal expansion in-plane is complicated by the fact that faces and core have different expansion coefficients, but being bonded together, they are forced

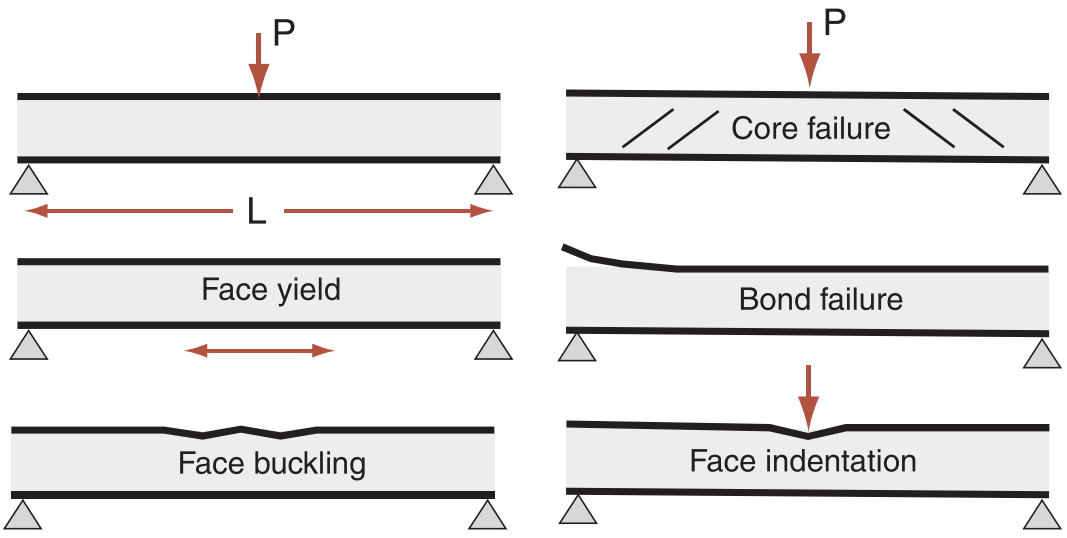

Figure 13.17 Failure modes of sandwich panels.

to suffer the same strain. This constraint leads to an in-plane expansionc coefficient of

$$\tilde{\alpha}_{//} = \frac{2tE_f\alpha_f + cE_c\alpha_c}{2tE_f + cE_c} \tag{13.21}$$

The through-thickness coefficient is simpler; it is given by the weighted mean

$$\tilde{\alpha}_{\perp} = \frac{2t\alpha_f + c\alpha_c}{2t + c} \tag{13.22}$$

Through-thickness thermal diffusivity is not a single-valued quantity, but depends on time. At short times heat does not penetrate the core and the diffusivity is that of the face, but at longer times the diffusivity tends to the value given by the ratio $\tilde{\lambda}/\tilde{\rho}\tilde{C}_p$.

Electrical properties. The dielectric constant of a sandwich, as with composites, is given by a rule of mixtures, equation (13.12) with $f = 2t/d$. Because the core is usually a foam, this allows the construction of stiff, strong sandwich shells with exceptionally low dielectric loss. In-plane electrical conductivity, too, follows such a rule. Through-thickness conductivity, like that of heat, is described by the harmonic mean (the equivalent of equation (13.20)).

13.6 Lattices: hybrids of type 3

Lattices — foams and other cellular structures — are hybrids of a solid and a gas. The properties of the gas might at first sight seem irrelevant, but this is not so. The thermal conductivity of low-density foams of the sort used for insulation is determined by the conductivity of the gas; and the dielectric constant and breakdown potential, and even the compressibility, depend on the gas properties. We therefore think of lattices as hybrids, and calculate their properties in the way shown in Figure 13.18.

There are two distinct species of cellular solid. The distinction is most obvious in their mechanical properties. The first, typified by foams, are *bending-dominated structures*; the second, typified by triangulated lattice structures, are *stretch dominated* — a distinction explained more fully below. To give an idea of the difference: a foam with a relative density of 0.1 (meaning that the solid cell walls occupy 10% of the volume) is less stiff by a factor of 10 than a triangulated lattice of the same relative density. The word "configuration" has special relevance here.

Bending dominated structures

Figure 13.19 shows an idealized cell of a low-density foam. It consists of solid cell walls or edges surrounding a void space containing a gas or fluid. Cellular

solids are characterized by their relative density, which for the structure shown here (with $t \ll L$) is

$$\frac{\tilde{\rho}}{\rho_s} = \left(\frac{t}{L}\right)^2 \tag{13.23}$$

where $\tilde{\rho}$ is the density of the foam, ρ_s is the density of the solid of which it is made, L is the cell size, and t is the thickness of the cell edges.

Mechanical properties. Figure 13.20 shows the compressive stress–strain curve of bending-dominated foams. The material is linear elastic, with modulus $\tilde{E}$ up to its elastic limit, at which point the cell edges yield, buckle or fracture. The foam continues to collapse at a nearly constant stress (the "plateau

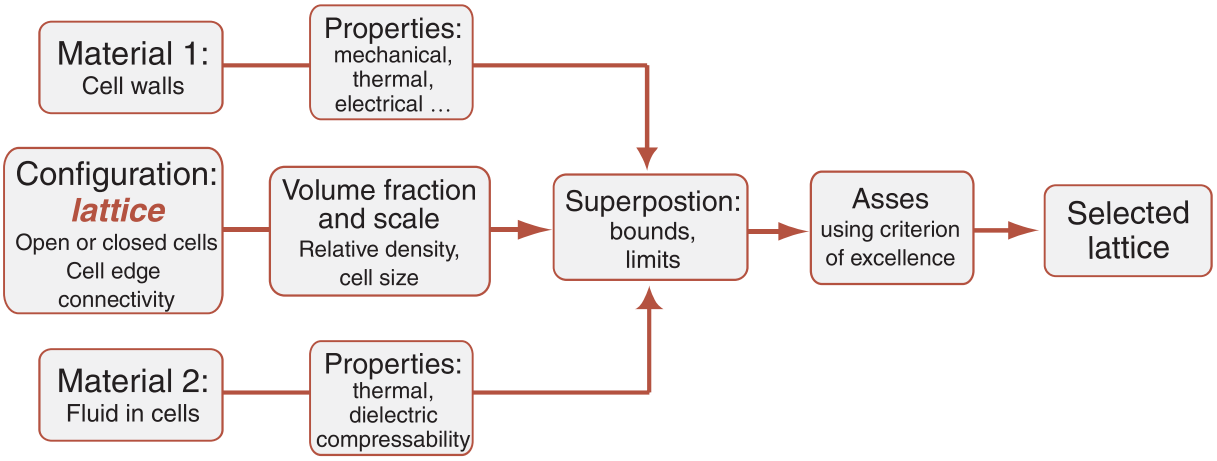

Figure 13.18 Foams and lattice structures: the design variables. They include the choice of material for the cell walls, the gas within the cells, the relative density, the cell size and shape, and — importantly — the connectivity of the cell edges.

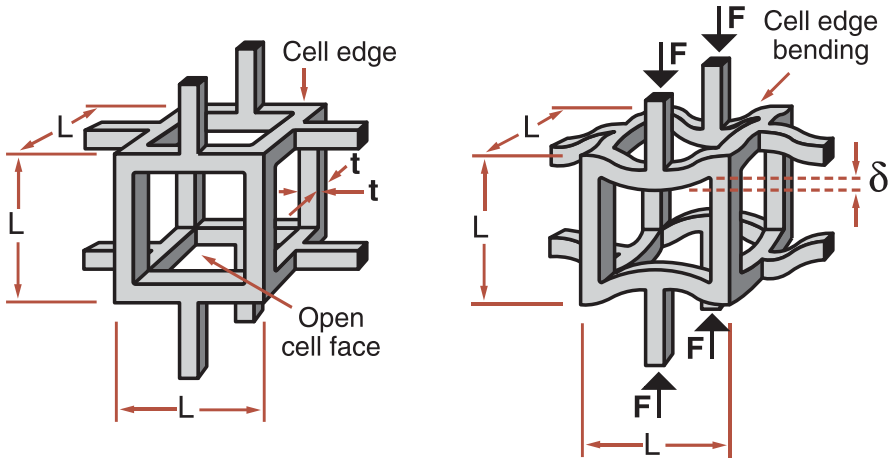

Figure 13.19 A cell in a low-density foam. When the foam is loaded, the cell edges bend, giving a low-modulus structure.

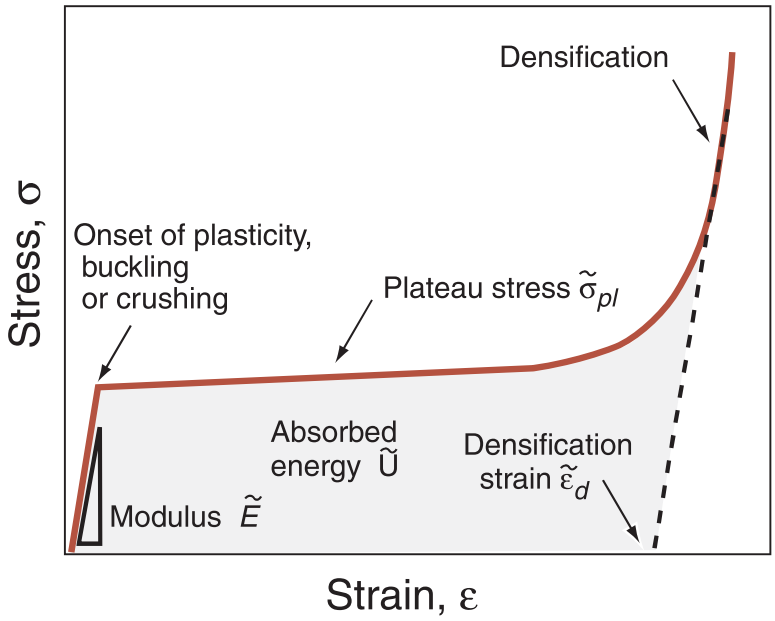

Figure 13.20 The plateau stress is determined by buckling, plastic bending or fracturing of the cell walls.

stress", $\tilde{\sigma}$) until opposite sides of the cells impinge (the "densification strain" $\tilde{\varepsilon}_d$), when the stress rises rapidly. The mechanical properties are calculated in the ways developed below, details of which can be found in the texts listed under Further reading. All are based on an idealized cell shape; real cells are less perfect than this, so the results should be regarded as upper bounds. Experiments show, however, that the results of the models give a good description of real foams.

A remote compressive stress σ exerts a force $F \propto \sigma L^2$ on the cell edges, causing them to bend and leading to a bending deflection δ, as shown in Figure 13.19. For the open-celled structure shown in the figure, the bending deflection is given by

$$\delta \propto \frac{FL^3}{E_s I} \tag{13.24}$$

where E_s is the modulus of the solid of which the foam is made and $I = (t^4/12)$ is the second moment of area of the cell edge of square cross section, $t \times t$. The compressive strain suffered by the cell as a whole is then $\varepsilon = 2\delta/L$. Assembling these results gives the modulus $\tilde{E} = \sigma/\varepsilon$ of the foam as

$$\frac{\tilde{E}}{E_s} \propto \left(\frac{\tilde{\rho}}{\rho_s}\right)^2 \quad \text{(bending-dominated behavior)} \tag{13.25}$$

Since $\tilde{E} = E_s$ when $\tilde{\rho} = \rho_s$ we expect the constant of proportionality to be close to unity—a speculation confirmed both by experiment and by numerical simulation.

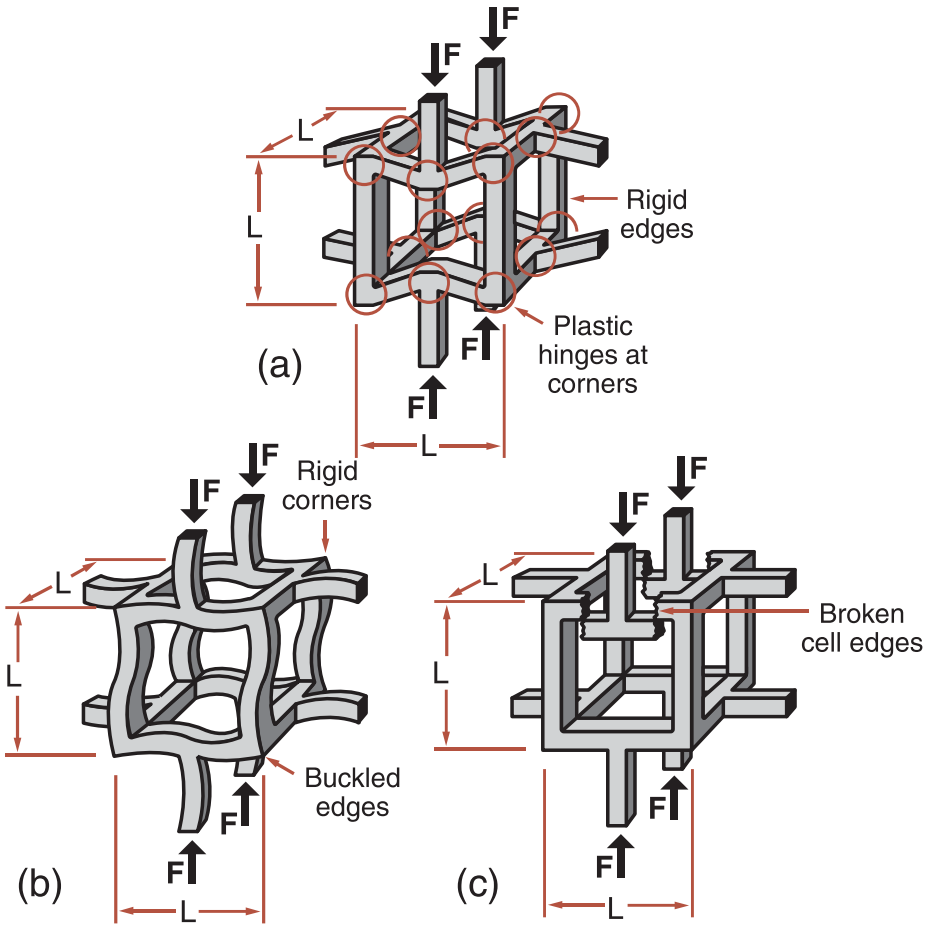

Figure 13.21 Collapse of foams. (a) When a foam made of a plastic materials loaded beyond its elastic limit, the cell edges bend plastically. (b) An elastomeric foam, by contrast, collapses by the elastic buckling of its cell edges. (c) A brittle foam collapses by the successive fracturing of cell edges.

A similar approach can be used to model the collapse, and thus the plateau stress of the foam. The cell walls yield, as shown in Figure 13.21(a) when the force exerted on them exceeds their fully plastic moment

$$M_f = \frac{\sigma_s t^3}{4} \tag{13.26}$$

where σ_s is the yield strength of the solid of which the foam is made. This moment is related to the remote stress by $M \propto FL \propto \sigma L^3$. Assembling these results gives the failure strength $\tilde{\sigma}_{pl}$:

$$\frac{\tilde{\sigma}_{pl}}{\sigma_{y,s}} = C\left(\frac{\tilde{\rho}}{\rho_s}\right)^{3/2} \quad \text{(bending-dominated behavior)} \tag{13.27}$$

where the constant of proportionality, $C \approx 0.3$, has been established both by experiment and by numerical computation.

Elastomeric foams collapse not by yielding but by elastic bucking; brittle foams by cell-wall fracture (Figure 13.21(b) and (c)). As with plastic collapse,

simple scaling laws describe this behavior well. Collapse by buckling occurs when the stress exceeds $\tilde{\sigma}_{el}$, given by

$$\frac{\tilde{\sigma}_{el}}{E_s} \approx 0.05\left(\frac{\tilde{\rho}}{\rho_s}\right)^2 \tag{13.28}$$

and by cell wall fracture when it exceeds $\tilde{\sigma}_{cr}$, where

$$\frac{\tilde{\sigma}_{cr}}{\sigma_{cr,s}} \approx 0.3\left(\frac{\tilde{\rho}}{\rho_s}\right)^{3/2} \tag{13.29}$$

where $\sigma_{cr,s}$ is the modulus of rupture of the cell-wall material. Densification, when the stress rises rapidly, is a purely geometric effect: the opposite sides of the cells are forced into contact and further bending or buckling are not possible. It is found to occur at a strain $\tilde{\varepsilon}_d$ (the densification strain) of

$$\tilde{\varepsilon}_d = 1 - 1.4\left(\frac{\tilde{\rho}}{\rho_s}\right) \tag{13.30}$$

Foams are often used for cushioning, packaging or to protect against impact. The useful energy that a foam can absorb per unit volume is approximated by

$$\tilde{U} \approx \tilde{\sigma}\tilde{\varepsilon}_d \tag{13.31}$$

where $\tilde{\sigma}$ is the plateau stress — the yield, buckling or fracturing strength of the foam, whichever is least.

This behavior is not confined to open-cell foams with the structure idealized in Figure 13.19. Most closed-cell foams also follow these scaling laws, at first sight an unexpected result because the cell faces must carry membrane stresses when the foam is loaded, and these should lead to a linear dependence of both stiffness and strength on relative density. The explanation lies in the fact that the cell faces are very thin; they buckle or rupture at stresses so low that their contribution to stiffness and strength is small, leaving the cell edges to carry most of the load.

Thermal properties. The specific heat of foams, when expressed in units of $J/m^3\,K$, is given by a rule of mixtures, summing the contributions from the solid and the gas. The thermal expansion coefficient of an open cell foam is the same as that of the solid from which it is made. The same is true of rigid closed-cell foams but not necessarily of low density elastomeric foams because the expansion of the gas within the cells can expand the foam itself, giving an apparently higher coefficient.

The cells in most foams are sufficiently small that convection of the gas within them is completely suppressed. The thermal conductivity of the foam is thus the sum of that conducted through the cell walls and that through the still air (or other gas) they contain. To an adequate approximation

$$\tilde{\lambda} = \frac{1}{3}\left(\left(\frac{\tilde{\rho}}{\rho_s}\right) + 2\left(\frac{\tilde{\rho}}{\rho_s}\right)^{3/2}\right)\lambda_s + \left(1 - \left(\frac{\tilde{\rho}}{\rho_s}\right)\right)\lambda_g \tag{13.32}$$

where λ_s is the conductivity of the solid and λ_g that of the gas (for dry air it is 0.025 W/m.K). The term associated with the gas is important: blowing agents for foams intended for thermal insulation are chosen to have a low value of λ_g.

Electrical properties. Insulating foams are attractive for their low dielectric constant, falling towards 1 (the value for air or vacuum) as the relative density decreases:

$$\tilde{\varepsilon} = 1 + (\varepsilon_s - 1)\left(\frac{\tilde{\rho}}{\rho_s}\right) \tag{13.33}$$

where ε_s is the dielectric constant of the solid of which the foam is made. The electrical conductivity follows the same scaling law as the thermal conductivity.

Stretch-dominated structures

If conventional foams have low stiffness because the configuration of their cell edges allows them to bend, might it not be possible to devise other configurations in which the cell edges were made to stretch instead? This thinking leads to the idea of *micro-truss lattice-structures*. To understand these we need one of those simple yet profound fundamental laws: it is the Maxwell stability criterion.

The condition that a pin-jointed frame (meaning one that is hinged at its corners) made up of b struts and j frictionless joints, like those in Figure 13.22

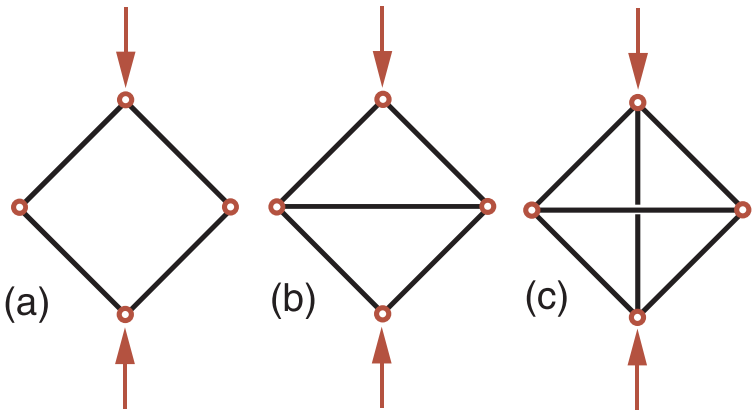

Figure 13.22 The pin-jointed frame at (a) folds up when loaded — it is a mechanism. If its joints are welded together, the cell edges bend (as in Figure 13.16) — it becomes a *bending-dominated structure*. The pin-jointed, triangulated, frame at (b) is stiff when loaded because the transverse bar carries tension, preventing collapse. When its joints are welded its stiffness and strength hardly change because it is a *stretch-dominated structure*. The frame at (c) is over-constrained. If the horizontal bar is tightened, the vertical one is put in tension even when there are no external loads: a state of *self-stress* exists.

to be both statically and kinematically determinate (meaning that it is rigid and does not fold up when loaded) in two dimensions, is

$$M = b - 2j + 3 = 0 \tag{13.34}$$

In three dimensions the equivalent equation is

$$M = b - 3j + 6 = 0 \tag{13.35}$$

If $M < 0$, the frame is a *mechanism*. It has no stiffness or strength; it collapses if loaded. If its joints are locked, preventing rotation (as they are in a lattice) the bars of the frame *bend* when the structure is loaded, just as in Figure 13.19. If, instead, $M \geq 0$ the frame ceases to be a mechanism. If it is loaded, its members carry tension or compression (even when pin-jointed), and it becomes a *stretch-dominated* structure. Locking the joints now makes little difference because slender structures are much stiffer when stretched than when bent. There is an underlying principle here: *stretch dominated structures have high structural efficiency; bending dominated structures have low.*

Mechanical properties. These criteria give a basis for the design of efficient micro-truss structures. For the cellular structure of Figure 13.19, $M < 0$, and bending dominates. For the structure shown in Figure 13.23, however, $M > 0$ and it behaves as an almost isotropic, stretch-dominated structure. On average one third of its bars carry tension when the structure is loaded in simple tension, regardless of the loading direction. Thus

$$\frac{\tilde{E}}{E_s} \approx \frac{1}{3}\left(\frac{\tilde{\rho}}{\rho_s}\right) \quad \text{(isotropic stretch-dominated behavior)} \tag{13.36}$$

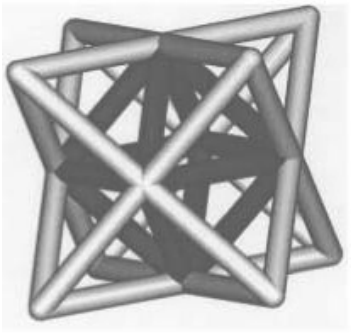

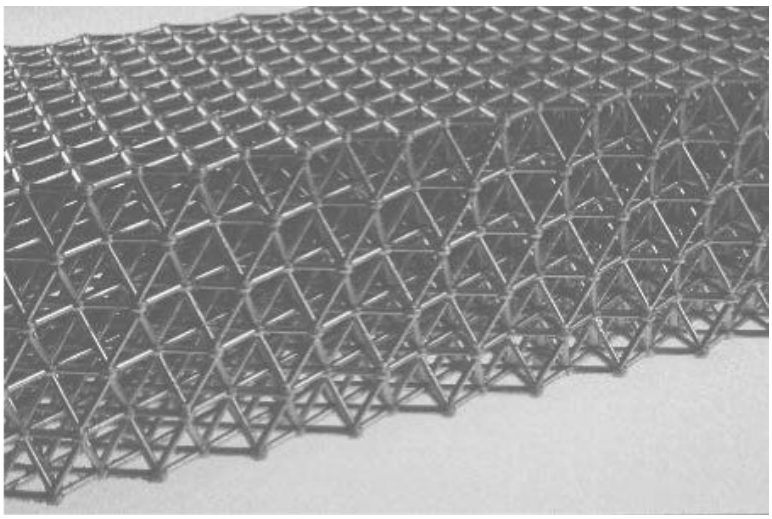

Figure 13.23 A micro-truss structure and its unit cell. This is a stretch dominated structure, and it is over-constrained, meaning that it is possible for it to be in a state of self-stress.

and its collapse stress is

$$\frac{\tilde{\sigma}}{\sigma_{y,s}} \approx \frac{1}{3}\left(\frac{\tilde{\rho}}{\rho_s}\right) \quad \text{(isotropic stretch-dominated behavior)} \tag{13.37}$$

This is an upper bound since it assumes that the struts yield in tension or compression when the structure is loaded. If the struts are slender, they may buckle before they yield. Then the "strength", like that of a buckling foam (equation (13.28)), is

$$\frac{\tilde{\sigma}_{el}}{E_s} \approx 0.2\left(\frac{\tilde{\rho}}{\rho_s}\right)^2 \tag{13.38}$$

These results are summarized in Figure 13.24 in which the modulus $\tilde{E}$ is plotted against the density $\tilde{\rho}$. Stretch dominated, prismatic microstructures have moduli that scale as $\tilde{\rho}/\rho_s$ (slope 1); bending dominated, cellular, microstructures have moduli that scale as $(\tilde{\rho}/\rho_s)^2$ (slope 2). Given that the density can be varied through a wide range, this allows great scope for material design. Note how the use of microscopic shape has expanded the occupied area of $E - \rho$ space.

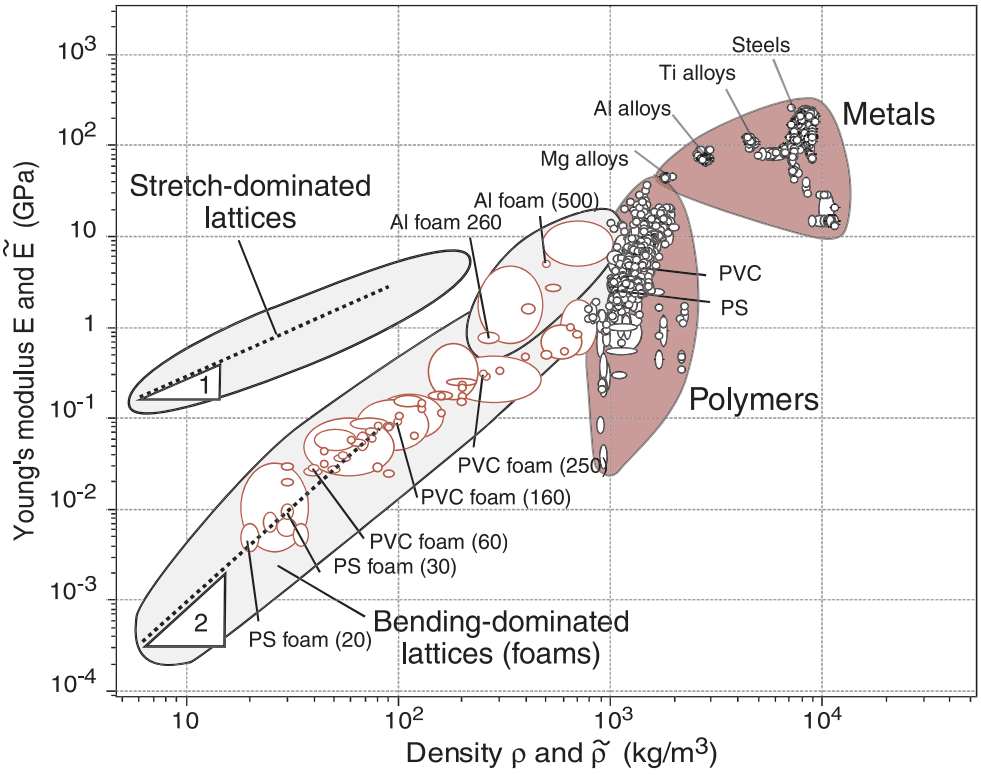

Figure 13.24 Foams and micro-truss structures are hybrids of material and space. Their mechanical response depends on their structure. Foams are usually bending dominated (equations (13.25) and (13.27)), and lie along a line of slope 2 on this chart. Micro-truss structures are stretch-dominated (equations (13.36) and (13.37)) and lie on a line of slope 1. Both extend the occupied area of this chart by many decades.

Thermal and electrical properties. The bending/stretching distinction influences mechanical properties profoundly, but has no effect on thermal or electrical properties, which are adequately described by the equations listed above for foams.

13.7 Segmented structures: hybrids of type 4

"United we stand, divided we fall" as the saying goes. But if "falling" means bending or twisting easily, it is something we sometimes want. And division is the way to get it (Figure 13.25).

Subdivision as a design variable

Shape can be used to reduce flexural stiffness and strength as well as increase them. Springs, suspensions, flexible cables and other structures that must flex yet have high tensile strength, use shape to give a low bending stiffness. This is achieved by shaping the material into strands or leaves, as suggested in Figure 13.26. As explained in Chapter 12, Section 12.8, the slender strands or leaves bend easily but do not stretch when the section is bent: an n-strand cable is less stiff by a factor of $3/\pi n$ than the solid reference section; an n-leaf panel by a factor $1/n^2$.

Subdivision can be used in another way: to impart *damage tolerance*. A glass window, hit by a projectile, will shatter. One made of small glass bricks, laid as bricks usually are, will lose a brick or two but not shatter totally; it is damage-tolerant. By sub-dividing and separating the material, a crack in one segment does not penetrate into its neighbors, allowing local but not global failure. That is the principle of "topological toughening". Builders in stone and brick have exploited the idea for thousands of years: both materials are brittle, but buildings made of them — even those made without cement ("dry-stone

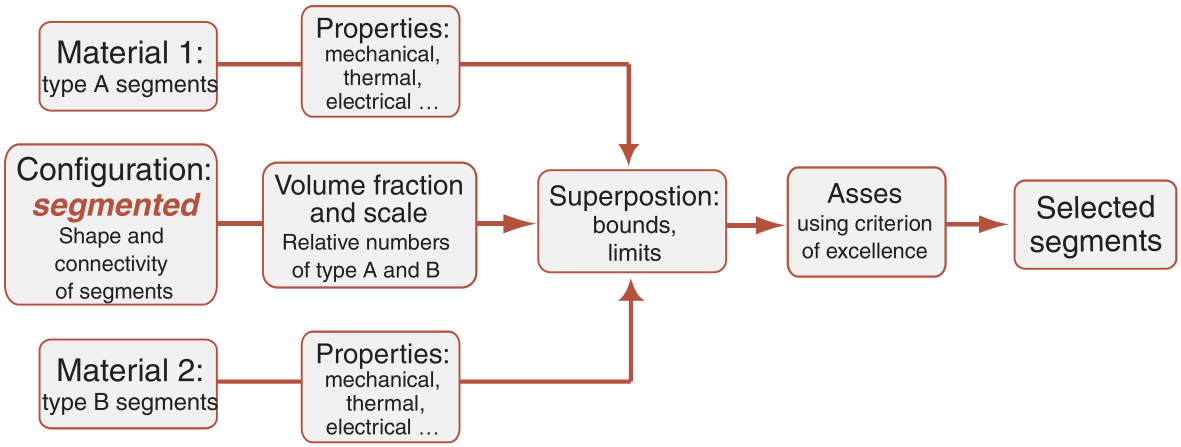

Figure 13.25 Segmented structures: the design variables. They include the choice of materials for the segments, and their shape, size, and stacking.

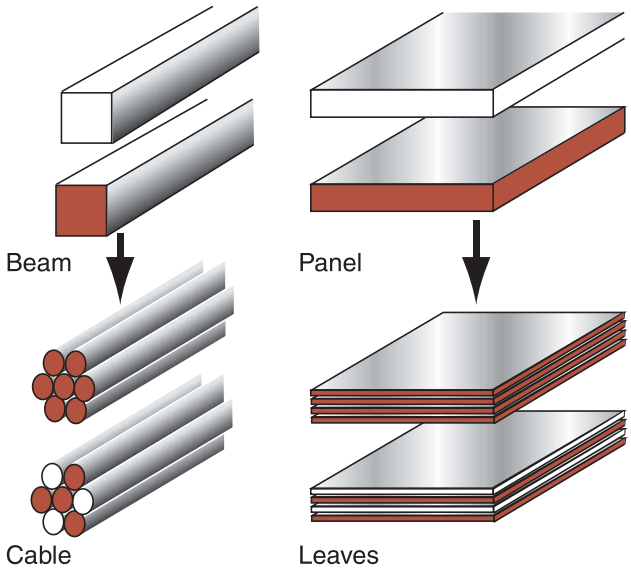

Figure 13.26 Making low-efficiency structures. Shape gives the sections a lower flexural stiffness and strength per unit mass than the solid section from which they are made.

building")—survive ground movement, even earthquakes, through their ability to deform with some local failure but without total collapse.

Taking the simplest view, two things are necessary for topological damage tolerance: discreteness of the structural units, and an interlocking of the units in such a way that the array as a whole can carry load. Brick-like arrangements (Figure 13.27a) carry large loads and are damage tolerant in compression and shear, but disintegrate under tension. Strand and layer like structures are damage-tolerant in tension because if one strand fails the crack does not penetrate its neighbors—the principle of multi-strand ropes and cables. The jigsaw puzzle configuration (Figure 13.27b) carries in-plane tension, compression and shear, but at the cost of introducing a stress concentration factor of about, $\sqrt{R/r}$, where R is the approximate radius of a unit and r that of the interlock. Dyskin and his colleagues (see Further reading) explore a particular set of topologies that rely on compressive or rigid boundary conditions to create continuous layers that tolerate out-of-plane forces and bending moments, illustrated in Figure 13.27c. This is done by creating interlocking units with non-planar surfaces that have curvature both in the plane of the array and normal to it. Provided the array is constrained at its periphery, the nesting shapes limits the relative motion of the units, locking them together. Topological interlocking of this sort allows the formation of continuous layers that can be used for ceramic claddings or linings to give surface protection. And of course the units need not be made of one material alone. Since the only requirement is that of interlocking shape, the segments can be made of different materials. Just as builder constructing a brick wall can insert porous bricks for ventilation and transparent bricks to admit light, the designer of a segmented hybrid can add functionality through the choice of material for the units.

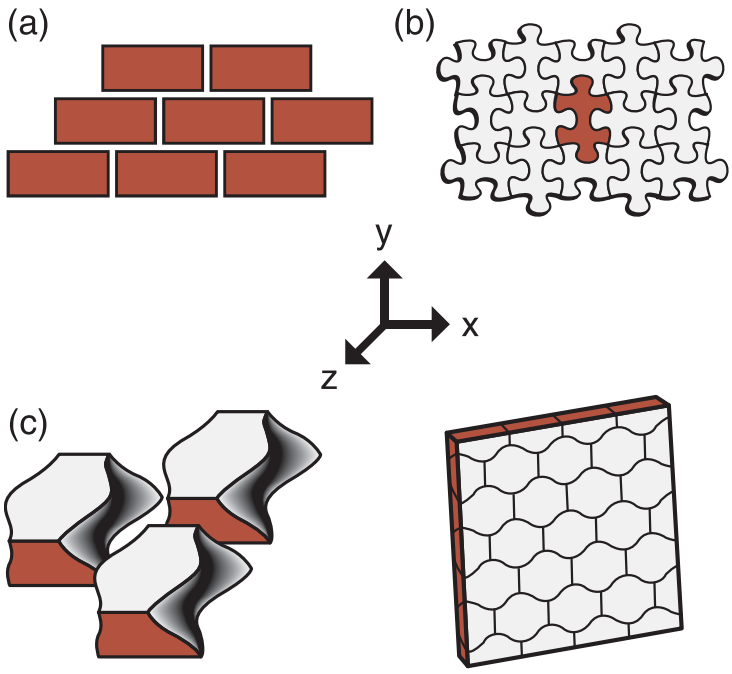

Figure 13.27 Examples of topological interlocking: discrete, unbonded structures that carry load. (a) Brick-like assemblies of rectangular blocks carry axial compression, but not tension or shear. (b) The two-dimensional interlocking of a jig-saw puzzle carries in-plane loads. (c) The units suggested by Dyskin *et al.* (2001), when assembled into a continuous layer and clamped within a rigid boundary around its edge, can carry out-of-plane loads and bending moments.

The in-plane compression modulus and strength of any of the arrays of Figure 13.27 are simply equal to those of the solid of which the segments are made, combined as a rule of mixtures if more than one material is used to make them. The in-plain tensile modulus and strength reflect the characteristics of the peripheral constraint. More interesting are the those for bending. Figure 13.28 shows schematically what happens when the array (reduced to just two segments for simplicity) is subjected to a load W/unit depth, causing a deflection δ. A peripheral constraining force, T per unit depth, holds them together. Let T have the generalized form

$$T = T_0 + 2\,\Delta d S^* \tag{13.39}$$

Here T_0 is the pre-tension and the constraining stiffness S^* describes how T increases as the blocks are wedged apart by the distance Δd per block:

$$\Delta d = \frac{b}{d}\delta$$

The lower figure shows a rigid body diagram for one block. Taking moments about the point A gives the force-displacement response

$$\widetilde{W} = \frac{2(b-\delta)}{d}\left(T_0 + 2S^*\frac{(b-\delta)\delta}{d}\right) \tag{13.40}$$

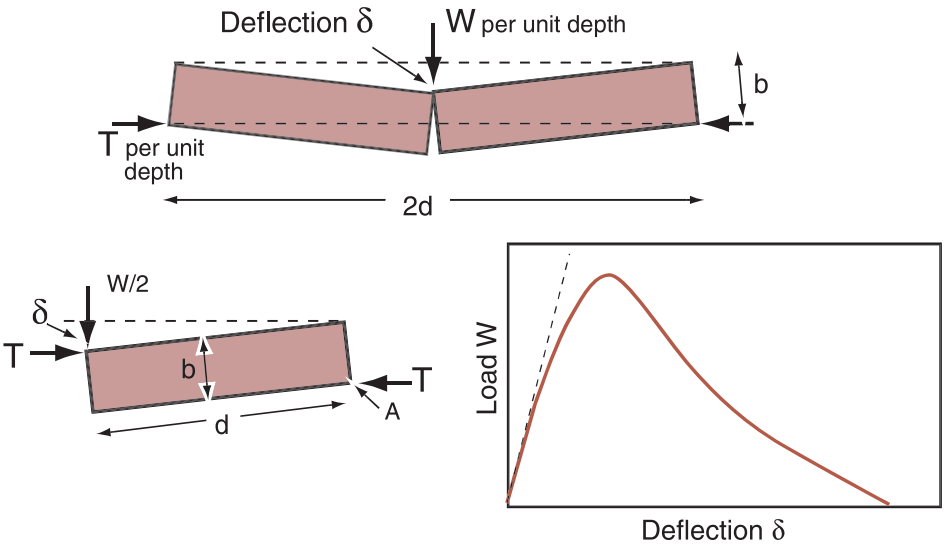

Figure 13.28 The loading on a pair of segments with the free-body diagram for one of them, and the flexural load-deflection response for the constrained segments.

If $S^* = 0$ the array is unstable when $\widetilde{W} > (2b/d)T_0$. If instead $T_0 = 0$ and $S^* > 0$,

$$\widetilde{W} = 4S^* \frac{(b-\delta)\delta}{d}$$

and the array shows linear-elastic response at small δ, becoming unstable at $\delta = b/3$. The behavior is sketched on the right of Figure 13.28.

The damage tolerance can be understood in the following way. We suppose that the units of the structure are all identical, each with a volume V_s, and that they are assembled into a body of volume V_t; there are therefore $n = V_t/V_s$ segments. We describe the probability of failure of a segment under a uniform tensile stress σ by a Weibull probability function:

$$P_f(V,\sigma) = 1 - \exp -\left\{\frac{V\sigma^m}{V_0\sigma_0^m}\right\} \tag{13.41}$$

where m, V_0 and σ_0 are constants. If the body were made of a single monolithic piece of the brittle solid, this equation, with $V = V_t$ would describe the failure probability. To calculate the design stress σ_t^* we set an acceptable value for P, which we call P^* (say 10^{-6}, meaning that it is acceptable if one in a million fail) and invert the equation to give

$$\sigma_t^* = \sigma_0\left\{\frac{V_0}{V_t}\ln(1-P^*)\right\}^{1/m} \tag{13.42}$$

Now consider the segmented body. A remote stress, if sufficiently large, causes some segments to fail. We refer to the fraction that has failed as the *damage*, D. If loaded such that each segment carried a uniform stress σ the

damage is simply $p_f(V_s, \sigma)$. If some segments fail the body as a whole remains intact; global failure requires that a fraction D^*, the critical damage (say, 10%), must fail. Inverting equation (13.41) with $V = V_s$ gives the global failure stress σ_s^* of the segmented body:

$$\sigma_s^* = \sigma_0 \left\{ \frac{V_0}{V_s} \ln(1 - D^*) \right\}^{1/m} \tag{13.43}$$

Thus segmentation increases the allowable design stress from σ_t^* to σ_s^*, a factor of

$$\frac{\sigma_s^*}{\sigma_t^*} = \left\{ n \frac{\ln(1 - D^*)}{\ln(1 - P^*)} \right\}^{1/m} \approx \left\{ n \frac{D^*}{P^*} \right\}^{1/m} \tag{13.44}$$

(expanding the logarithm as a series and retaining the first term — an acceptable approximation for small P^* and D^*). Both n and D^*/P^* are considerably greater than 1, so the equation suggests that segmentation always increases the design stress.

The merit of this argument is its simplicity, illustrating how damage tolerance can arise. But it is a little too simple. What are the underlying assumptions? First, that the number of segments is large; only then can the damage D be reliably equated to the failure probability P_f. Second, that the stress σ is uninfluenced by damage; in reality its average value increases by the factor $1/(1 - D)$. Third, that the stress is uniform; in reality both the interlocking shapes and the load shed by a failed segment onto its immediate neighbors increases the stresses locally by a effective stress concentration factor K_c. And fourth, that segment failure is uncorrelated ("non-associated cracking"), not linked ("associated cracking"). The first of these is simply a pre-condition that must be met for segmentation to be successful. The second and third of these can be included approximately by modifying equation (13.44) to give:

$$\frac{\sigma_s^*}{\sigma_t^*} \approx \left(\frac{1 - D}{K_c} \right) \left\{ n \frac{D^*}{P^*} \right\}^{1/m} \tag{13.45}$$

The last depends on the values of the Weibull constants, and requires numerical modeling to explore the conditions for non-associated cracking. Equation (13.45) however is still useful — it allows for both a gain and a loss in allowable design stress.

Figure 13.29 gives an idea of the messages that it carries. It is constructed using $K_c = 2$, and values of nD^*/P^* between 10^4 and 10^{10}. The Weibull modulus m of brittle solids typically lies in the range 5 (typical of a porous brittle ceramic) and 30 (a value that might describe the variability of a high technical ceramic). When the Weibull modulus is large — more than 25 — segmentation offers little gain, indeed there may be a loss of allowable stress. But when it is low (as it is in building materials like brick and stone, and as it can be for

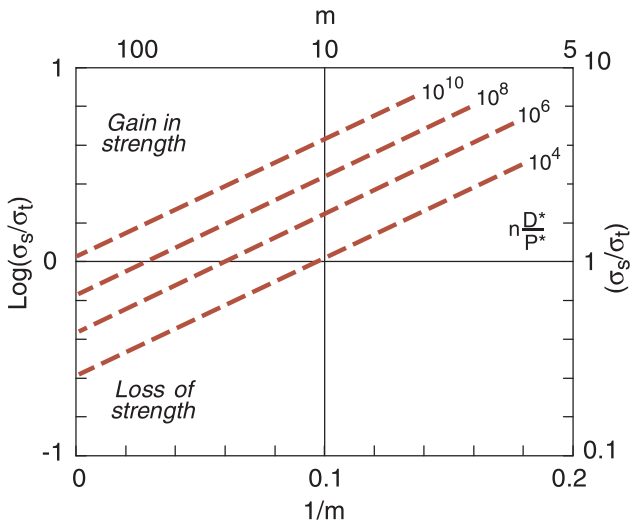

Figure 13.29 The ratio σ_s/σ_t for the listed values of nD^*/P^*, with $K_c = 2$ and $D^* = 0.1$.

certain ceramics and glasses) there is a gain. Segmentation gives a new design variable.

13.8 Summary and conclusions

The properties of engineering materials can be thought of as defining the axes of a multi-dimensional space with each property as a dimension. Sections through this space can be mapped. These maps reveal that some areas of property-space are occupied, others are empty — there are holes. The holes can sometimes be filled by making hybrids: combinations of two (or more) materials in a chosen configuration and scale. Design requirements isolate a small box in a multi-dimensional material–property space. If it is occupied by materials, the requirements can be met. But if it hits a hole in any one of the dimensions, we need a hybrid. A number of families of configuration exist, each offering different combinations of functionality. Each configuration is characterized by a set of bounds, bracketing its effective properties. The methods developed in this chapter provide tools for exploring alternative material–configuration combinations. Chapter 14 gives examples of their use.

13.9 Further reading

Allen, H.G. (1969) *Analysis and Design of Structural Sandwich Panels*, Pergamon Press, Oxford, UK. *(The bible: the book that established the principles of sandwich design).*

Ashby, M.F. (1993) Criteria for selecting the components of composites, *Acta Mater.* **41**, 1313–1335. *(A compilation of models for composite properties, introducing the methods developed here.)*

Ashby, M.F., Evans, A.G., Fleck, N.A., Gibson, Lorna J., Hutchinson J.W. and Wadley, H.N.G. (2000) *Metal Foams: A Design Guide*, Butterworth-Heinemann, Oxford. ISBN 0-7506-7219-6. *(A text establishing the experimental and theoretical basis of the properties of metal foams, with data for real foams and examples of their applications.)*

Bendsoe, M.P. and Sigmund, O. (2003) *Topology Optimisation, Theory Methods and Applications*, Springer-Verlag, Berlin, Germany. ISBN 3-540-42992-1. *(The first comprehensive treatment of emerging methods for optimizing configuration and scale.)*

Chamis, C.C. (1987) in *Engineers Guide to Composite Materials*, pp. 3–8 — 3–24. Am. Soc. Metals, Materials Park, Ohio, USA. *(A compilation of models for composite properties.)*

Deshpande, V.S., Ashby, M.F. and Fleck, N.A. (2001) "Foam topology: bending versus stretching dominated architectures", *Acta Mater.* **49**, 1035–1040. *(A discussion of the bending vs. stretching dominated topologies.)*

Dyskin, A.V., Estrin, Y., Kanel-Belov, A.J. and Pasternak, E. (2001) "Toughening by fragmentation: how topology helps", *Advanced Engineering Materials* **3**, 885–888; (2003) "Topological interlocking of platonic solids: a way to new materials and structures", *Phil. Mag.* **83**, 197–203. *(Two papers that introduce interlocking configurations that carry bending loads, yet give damage tolerance.)*

Gibson, L.J. and Ashby, M.F. (1997) *Cellular Solids, Structure and Properties*, 2nd edition, Cambridge University Press, Cambridge, UK. ISBN 0-521-49560-1. *(A monograph analyzing the properties, performance and uses of foams and giving the derivations and experimental verification of the equations used in Section 13.6.)*

Schoutens, J.E. and Zarate, D.A. (1986) *Composites* **17**, 188. *(A compilation of models for composite properties.)*

Stauffer, D. and Aharony, A. (1994) *Introduction to Percolation Theory*, 2nd edition, Taylor and Francis, London UK. *(A personal but very readable introduction to percolation theory.)*

Watt, J.P., Davies, G.F. and O'Connell, R.J. (1976) *Rev. Geophys. Space Phys.* **14**, 541. *(A compilation of models for composite properties.)*

Weibull, W. (1951) *J. Appl. Mech.* **18**, 293. *(The orginator or the "weakest –link" model of a brittle solid.)*

Zenkert, D. (1995) *An Introduction to Sandwich Construction*, Engineering Advisory Services Ltd., Solihull, UK, published by Chameleon Press Ltd., London, UK. ISBN 0 947817778. *(A primer, aiming to teach the basic analysis of sandwich structures.)*

Chapter 14

Hybrid case studies

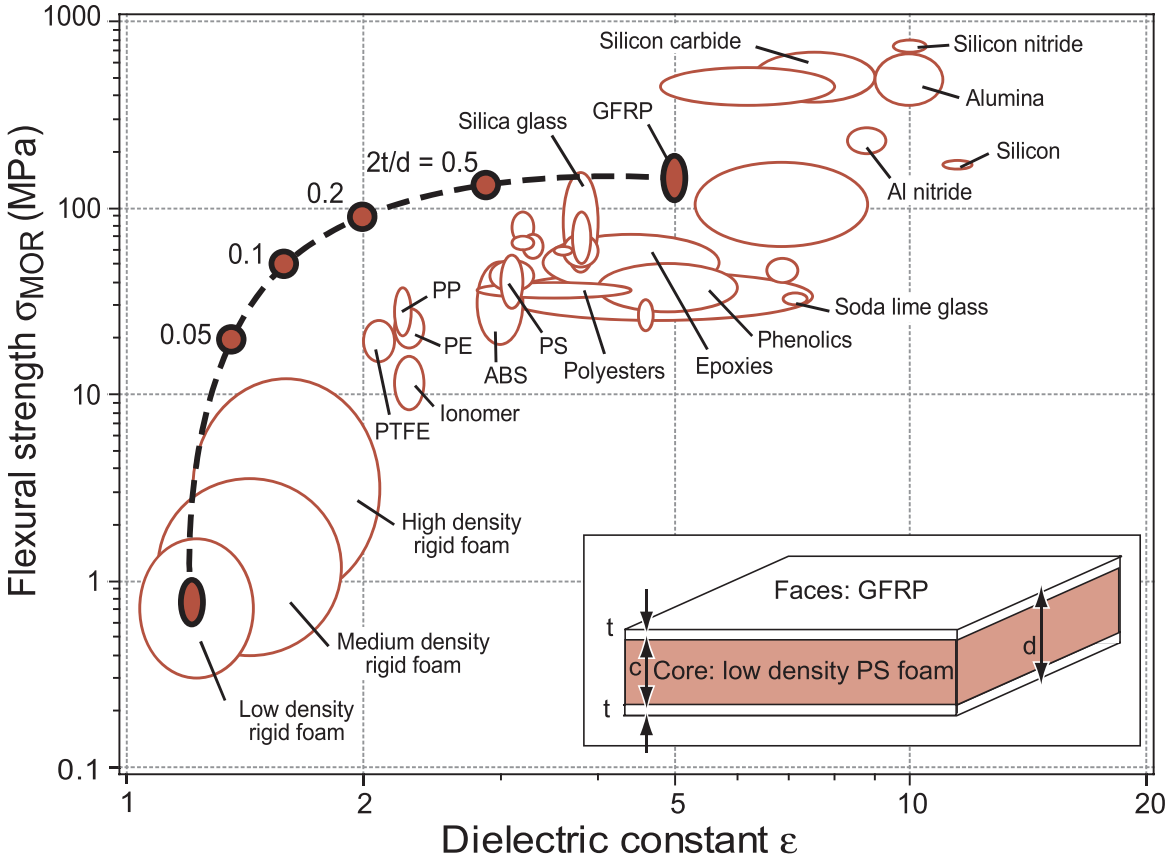

Chapter contents

14.1	Introduction and synopsis	380	14.6	Materials for microwave-transparent enclosures	389
14.2	Designing metal matrix composites	380	14.7	Exploiting anisotropy: heat spreading surfaces	391
14.3	Refrigerator walls	382	14.8	The mechanical efficiency of natural materials	393
14.4	Connectors that do not relax their grip	384	14.9	Further reading: natural materials	399
14.5	Extreme combinations of thermal and electrical conduction	386			